Master's thesis

NTNU
Norwegian University of Science and Technology
Faculty of Natural Sciences
Department of Physics

Maren Andrine Teien

Combining offshore wind power and hydrogen production

Assessment of storage requirements and energy utilization for different configurations

Master's thesis in Applied Physics and Mathematics
Supervisor: Magnus Korpås
June 2022

NTNU
Norwegian University of
Science and Technology

Maren Andrine Teien

Combining offshore wind power and hydrogen production

Assessment of storage requirements and energy utilization for different configurations

Master's thesis in Applied Physics and Mathematics
Supervisor: Magnus Korpås
June 2022

Norwegian University of Science and Technology
Faculty of Natural Sciences
Department of Physics

NTNU
Norwegian University of
Science and Technology

Summary

International energy goals require increased electrification and integration of renewable power. In Europe, there is an increased priority on integrating offshore wind, and the continent has a goal of installing 60 GW by 2030. In February 2022, the Norwegian Government announced the plan for a 1500 MW offshore wind power plant at Southern North Sea II, a suitable location for efficient power production and internal power supply. The Norwegian goal is to establish offshore wind with 30 GW capacity by 2040. Varying wind conditions and further the wind power production lead to varying power supply, and storing energy in the production of hydrogen gas can make the wind power more balanced. Hydrogen is also considered a replacement for fossil fuels in heavy industry and transport, where batteries become enormous. The International Renewable Energy Agency (IRENA) suggests that hydrogen will contribute to 12 % of the total energy consumption by 2050.

This thesis aims to investigate the potential of offshore wind power production supplying offshore hydrogen production and storage. It also investigates how varying intervals for continuous delivery to shore, storage size and the wind power capacity affect the power transmission in a connected grid. Both offshore wind and onshore hydrogen production are established technologies but have never been combined on a large scale offshore. A 1400 MW offshore wind power plant was modelled to investigate the wind power potential at Southern North Sea II. It supplied power to an offshore electrolyser connected to offshore storage and a gas cable that transports hydrogen gas to shore.

The performed calculations resulted in a mean monthly capacity factor of 60.25 % at the offshore wind farm. The constant yearly delivery to shore gave total hydrogen demanded storage capacity of 8,071 tons. Decreasing the interval for continuous delivery decreased the storage demand. The continuous monthly delivery to shore led to a storage demand of 2,231 tons, which is 70 % less than the constant yearly interval. Further, a decreasing storage capacity from 100 % to 10 % led to an increasing grid transmission of 30 % for the case with constant yearly delivery to shore. The upscaling of the wind power plant led to increased power transmission of approximately 70 % and a decreased hydrogen storage demand of 89 % for a continuous yearly delivery to the shore. The upscaling of the wind power plant led to a decreased storage capacity demand, only ~5 % power dumping and higher utilisation of the components. The same tendencies were repeated for the other interval cases.

The salt cavern storage potential in the North Sea is enormous. In the Norwegian Territory, is it possible to produce and store hydrogen that would serve Europe with a continuous delivery throughout a year which would be 385 times the hydrogen goal of 2030, the same energy amount as five times the world energy consumption.

There were many hours of free capacity in the power grid, even if the total hydrogen storage capacity decreased. The capacity could be utilised for other purposes offshore, like electrifying an oil and gas platform or connecting to an offshore grid. A further comparison of the economic and technical combination of the components in the model still remains. The salt cavern potential needs to be further investigated to get more reliable data on the potential storage capacity in the salt caverns in the Norwegian North Sea.

Sammendrag

Internasjonale energimål krever integrering av fornybar kraft i strømnettet. I Europa er etablering av offshore vind en prioritet, og kontinentet har som mål å installere 60 GW innen 2030. I februar i 2022 annonserte den norske regjeringen en plan om å installere 30 GW offshore vind innen 2040. Varierende vindforhold fører til varierende kraftproduksjon i et offshore vindkraftverk, og å lagre energi i hydrogengass kan være en del av løsningen for å gjøre vindkraft mer balansert. Hydrogen er også ansett som en mulig erstatter for fossilt brensel i tungindustri og stortransport, der batterier blir store og tunge. Det internasjonale fornybare energibyrået (IRENA) forventer at hydrogen vil være 12 % av verdens totale energiforbruk innen 2050.

Denne oppgaven har som mål å undersøke potensialet til havvindparker som kraftkilde til hydrogenproduksjon og -lagring offshore. Den har også som mål å undersøke hvordan varierende intervaller for konstant leveranse til land, endret lagringsstørrelse og endring av vindkapasiteten kan øke overføringen av kraft i det tilkoblede strømnettet. Både offshore vind og onshore hydrogenproduksjon har vært etablert i mange år, men har aldri blitt kombinert i storskala offshore. I denne oppgaven er en 1400 MW vindturbinpark modellert for å undersøke potensialet i Sørlige Nordsjø II. Den ga strøm til offshore hydrogenproduksjonsanlegg, som igjen var tilkoblet et offshore lagringsanlegg og et gassrørsystem som førte til land. Strømnettet ble senere tilkoblet for å studere hvordan overføringen varierte med varierende komponentstørrelser.

Kalkulasjonene av vindparken offshore resulterte i en gjennomsnittlig kapasitetsfaktor på 60.25 %. Konstant hydrogen leveranse til land hver time førte til et totalt lagerbehov på 8 071 tonn. Minkende intervall for konstant leveranse førte til mindre lagerbehov, og månedlig konstant leveranse ga et lagerbehov med 2 231 tonn, som er 70 % mindre enn det med årlig konstant intervall. En minkende lagerkapasitet fra 100 % til 10 % førte til en økende kraftoverføring i strømnettet på 70 % og et minkende lagerbehov av hydrogen på 89 % når det er konstant hydrogenleveranse til land, hele året. Oppskaleringen av vindkraftanlegget økte til mindre lagerbehov, bare ~5 % kraftdumping og høyere krafteksport, mindre kraft import og mindre størrelse på lagringsbehovet. Samme tendensen repeteres for de andre intervallcasene.

Hydrogenlagring i saltgruver i Nordsjøen har et enormt potensiale. I det norske territoriet er det mulig å produsere og lagre hydrogen som ville være med på å levere en konstant leveranse til Europa gjennom hele året som ville vært 385 ganger Europas hydrogenmål i 2030. Det er den samme energimengden som fem ganger hele verdens energibehov.

Selv om overføringen i strømnettet økte for en minkende lagringskapasitet, var det fortsatt mange timer med ledig kapasitet i strømnettet. Denne kapasiteten kan bli utnyttet til andre formål, som å elektrifisere en olje og gass plattform. Modellen med 2800 MW vindturbinpark utnyttet komponentene bedre, ved å eksportere mer strøm til strømnettet, og derfor både eksportere kraft og produsere hydrogenbehovet. Hydrogenlagring i saltgruver må studeres videre for å få mer pålitelige data som bekrefter lagringspotensiale i saltgruvene i Nordsjøen.

Preface

This master thesis is a part of the fifth year of Applied Physics and Mathematics at The Norwegian University of Science and Technology (NTNU) in Trondheim. It is a cooperation between The Department of Physics and The Department of Electrical Power Engineering at NTNU. This thesis investigates the potential of producing offshore hydrogen gas in the Norwegian North Sea with power supply from offshore wind. The background is the increased focus and optimism with hydrogen as a future green energy carrier. The basis of this thesis is in the project assignment written in December 2021, named *Case study on hydrogen production from offshore wind power*.

The master thesis has been achievable through excellent guidance from the supervisor, Magnus Korpås, at The Department of Electrical Power Engineering. Korpås has contributed with an essential and exciting insight into the field of study. The opportunity to combine a study background in Applied Physics with the field of sustainable power has been both exciting and educational. I will therefore thank Magnus Korpås for giving me this opportunity.

Maren Andrine Teien
Date: June 7, 2022

Contents

Acronyms

AC alternating current. 13, 26

AEL alcaline electrolysis. xi, 5, 6

ATM autothermal reforming. 4

CCS carbon capture and storage. 4

CCU carbon capture and utilisation. 4

CH_2 compressed hydrogen gas. 6, 7, 9

DC direct current. 13, 26

HVDC high voltage direct current. 26

LH_2 liquid hydrogen gas. 6, 7

NH_2 ammonia. 6, 7

OWT offshore wind turbines. 3

PEM protone exchange membrane. xi, 5, 6, 26

SMR steam methane reforming. 4

SNII Southern North Sea II. 25, 49

WPP wind power plant. viii, xi, 31, 35–37, 42, 44, 49, 51–53

List of Figures

List of Tables

This page was intentionally left blank.

1 Introduction

As the international renewable energy goals require sustainable power implementation, it is crucial to develop affordable low-carbon technologies [1]. In addition, industries dependent on fossil fuels, and society as a whole, are going through an electrification process that causes higher energy demand. Therefore, it is necessary to implement more sustainable power production in the following years.

The increasing energy demand has set offshore wind power production on the agenda. Europe has installed 27.8 GW of offshore wind in 2021 but has set a goal of installing 60 GW by 2030, and 300 GW by 2050 [2]. The North Sea is considered one of the best spots in Europe to integrate offshore wind power due to the suitable weather and water depth. Locating offshore wind power plants in the North Sea is an opportunity for efficient power production [3].

The United Kingdom and the Netherlands are examples of countries that look for possibilities for utilising the competence within the oil and gas industry and transferring it to offshore wind establishment and energy export. Norway has the same possibility, and competence [3]. Norway produces much of its electricity from hydropower, but the increased power demand requires new energy installations. By 2022, are no offshore wind installations established in the Norwegian territory of the North Sea. However, the Norwegian Government presented in February 2022 a plan to establish a 1500 MW offshore wind power plant in the Southern North Sea II (SNII) area [4]. The Norwegian Government's main goal is to produce 30 000 MW of offshore wind by 2040 [5].

Dependency on the weather and the following variations are challenging with renewable power production. Hydrogen gas production and storage from renewable power can secure more flexible and balancing energy systems. In addition, green hydrogen gas is often considered a possible replacement for fossil fuels in the industry and the transport sector. Hydrogen can potentially be the fuel of ships and heavy goods trucks where electrification and heavy batteries are impractical [3]. International Renewable Energy Agency (IRENA) suggested in their World Energy Transition Outlook that hydrogen will be 12 % of the world's energy consumption by 2050 [6]. Recently, more than 30 countries have launched their hydrogen strategies, and road maps [7]. Europe alone has set a goal of producing 10 million tons of green hydrogen gas each year from 2030 [3]. There is an already existing market for hydrogen gas, but the production account for around 830 million tons of CO_2-emissions annually [8]. A wind to hydrogen power plant could store variable renewable energy in the production of hydrogen gas and replace the hydrogen gas produced with CO_2-emissions.

A combination of offshore wind and hydrogen production has gotten increased attention in the last few years. Both the Norwegian Greenstat [3], Offshore Wind Industry Council & CATAPULT Offshore Renewable Energy [9], and the Scottish government [10] released articles comparing and considering offshore wind power production in combination with hydrogen production in the recent years.

Hydrogen is the most abundant element, the lightest and smallest, and storing hydrogen still faces many challenges. Embitterment in metal vessels is the main challenge, which leads to the demand of high-cost solutions. At the same time, pressure vessels are mobile and possible to place where ever. The International Energy Agency (IEA) stated in June 2019 that geological storage, namely salt caverns, depleted natural gas

or oil reservoirs, are the best options for large scale and long term storage [8]. Especially hydrogen storage in salt caverns is a promising option due to the low cost and cushion gas requirements.

This thesis aims to investigate the potential of offshore wind power production as a power source for offshore hydrogen production and storage in the North Sea territory. It also aims to study how transmission in a power grid connection changes when varying the intervals for continuous delivery, the hydrogen storage volume, and the wind power capacity. Hydrogen storage potential in salt caverns in the Norwegian North sea is also investigated. The model's base is an offshore wind power production to supply hydrogen production, located in the Southern North Sea II area. The wind to hydrogen model is extended by including a grid connection to the shore to optimise the wind to hydrogen power plant. The hydrogen storage potential in the Norwegian North Sea is calculated from a technical potential and further converted to energy units.

The basis of this master thesis is a project thesis written in December 2021, *Case study on hydrogen production from offshore wind power*. Some of the sections in this master thesis will overlap with the corresponding sections in the project thesis because of the similar subject.

2 Theory

2.1 Offshore wind turbines

Wind turbine technology has developed rapidly in the last decades, and the price of the technology has decreased at the same rate [3]. The capacity factor of offshore wind farms has increased due to technological improvements in recent years. The capacity factor is the number of hours the wind power produces at its maximum, compared to the total number of hours. The average capacity factor for offshore wind turbines (OWT) in Europe was 37 % in 2018. One of the newest projects with floating offshore turbines, Hywind Scotland, has a capacity factor of 53.8% [12]. There are two main groups of OWT, namely bottom-mounted and floating turbines. The offshore wind capacity in Europe was 25 GW by 2020, and only 0.25 % were floating turbines [13]. The technology of floating wind projects is still in an establishing phase, which affects the price and, therefore, the construction of those turbines [9]. A territory at sea is suitable for bottom-mounted turbines if the depth is less than 60 meters [14]. Otherwise, it is suitable with floating wind turbines. See figure 2.1 and identify the great potential for floating wind turbines in the North Sea due to the depth.

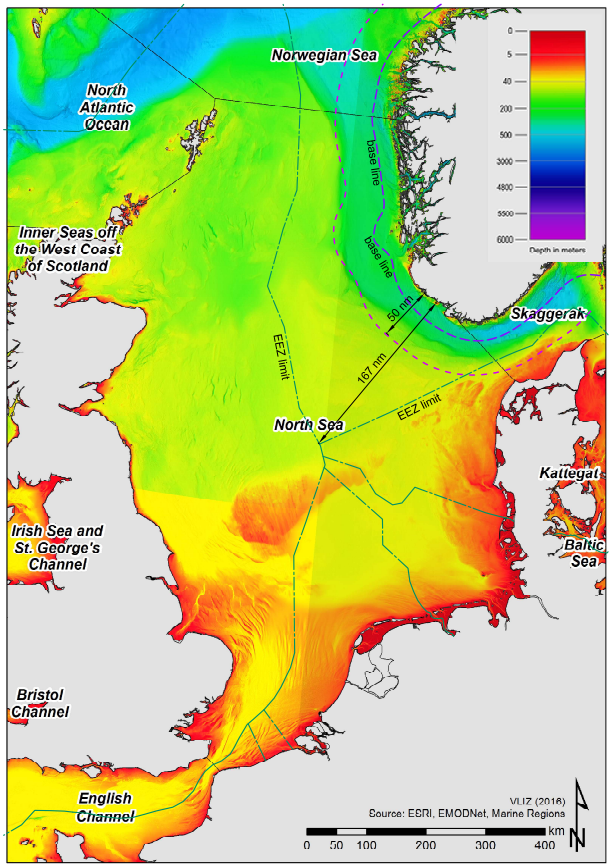

Figure 2.1: Map over the ocean depth in the North Sea. Yellow, green and blue colour indicate 40, 200 and 4000 m depth respectively [11]. This territory has a lot of areas with depth over 60 meters, and therefore a lot of potential capacity areas for establishing floating offshore wind turbines.

There are many variations of bottom-mounted offshore wind turbines, but the monopile and jacket structures are often considered and compared. See figure 2.2 for a visualisation of the main differences. By 2019, the monopile structure represented 81 % of all bottom-mounted turbines installed. The monopile structure is recommended for water depths up to 30 m, while the jacket foundation is a suitable foundation when water depths up to 60 m [15].

When an offshore wind power plant is established, is it necessary to place the turbines at a distinct minimal distance from each other in order to secure an optimal wind flow for an optimal power system [16]. The following equation shows the connection between the necessary area for a wind turbine, A_{WT}, and the wind turbine with rotor diameter, D_{rotor}

$$A_{WT} = (7 * D_{rotor})^2. \tag{2.1}$$

2.2 H_2-production

Hydrogen is one of the most promising energy carriers for a net-zero future. Hydrogen is not possible to find naturally, even though it is one of the most abundant element on planet earth [17]. Hydrogen gas is assigned a colour name to differentiate whether it is produced in a renewable or non-renewable way. The most common hydrogen products are Grey, Blue, Turquoise and Green Hydrogen. Figure 2.3 connect the colours with the production method and source.

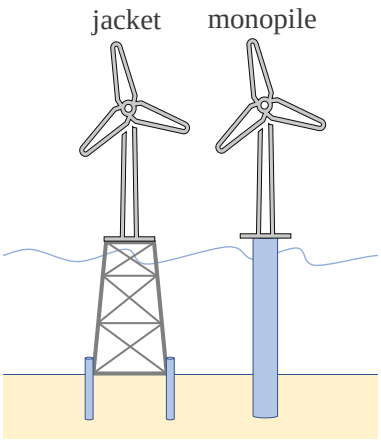

Figure 2.2: The main differences between jacket and monopile foundation structures.

Grey hydrogen is produced from fossil fuels by steam methane reforming (SMR) or autothermal reforming (ATM). The rest product is CO_2, and for every 1 kg of produced grey hydrogen gas, the system emits 10 kg of CO_2 [18]. The production of blue hydrogen is the same as grey hydrogen. The only difference is the emissions of CO_2 gas being either captured by carbon capture and storage (CCS) or used in the production of chemical raw materials or fuels called carbon capture and utilisation (CCU). The production of turquoise hydrogen is the pyrolysis of natural gas. The result is CO_2 in solid form, which can be utilised or buried. The electricity that provides the pyrolysis needs to come from renewable energy sources and capture the solid CO_2 to make turquoise hydrogen renewable. Electricity from renewable energy sources, like solar or wind power, supplies power to an electrolyser that produces green hydrogen. Green hydrogen is considered a possible replacement for fossil fuels in the industry and the transport sector and can potentially be the fuel of ships and heavy goods trucks where batteries are heavy and impractical [3].

2.2.1 Electrolysis

Electrolysis is already a mature technology that converts electric and thermal energy into chemical energy in the form of hydrogen gas. It uses water as a source and has only hydrogen and oxygen gas as by-products. When voltage is applied in an electrolysis cell, water molecules are divided into oxygen and hydrogen ions and later gathered into oxygen and hydrogen gas

$$\mathrm{H2O(l)} \rightarrow \mathrm{H2(g)} + \frac{1}{2}\,\mathrm{O2\,(g)}. \tag{2.2}$$

An electrolysis cell consists of an anode, a cathode, a diaphragm and an electrolyte. The connection of the electrolyte, anode and cathode creates a closed circuit after applying a direct current. The electrolyser needs the anode and cathode to resist corrosion and have good electric conductivity to operate optimally. The diaphragm is essential to prevent oxygen and hydrogen from reforming water and have a high electric conductivity to transport hydrogen ions. Water is injected at the anode side of the electrolysis cell. The oxygen ions create oxygen gas at the anode and hand over electrons, which travel through the voltage source. The hydrogen atoms travel through the diaphragm towards the cathode. Here, they create hydrogen gas with the incoming electrons at the cathode [17].

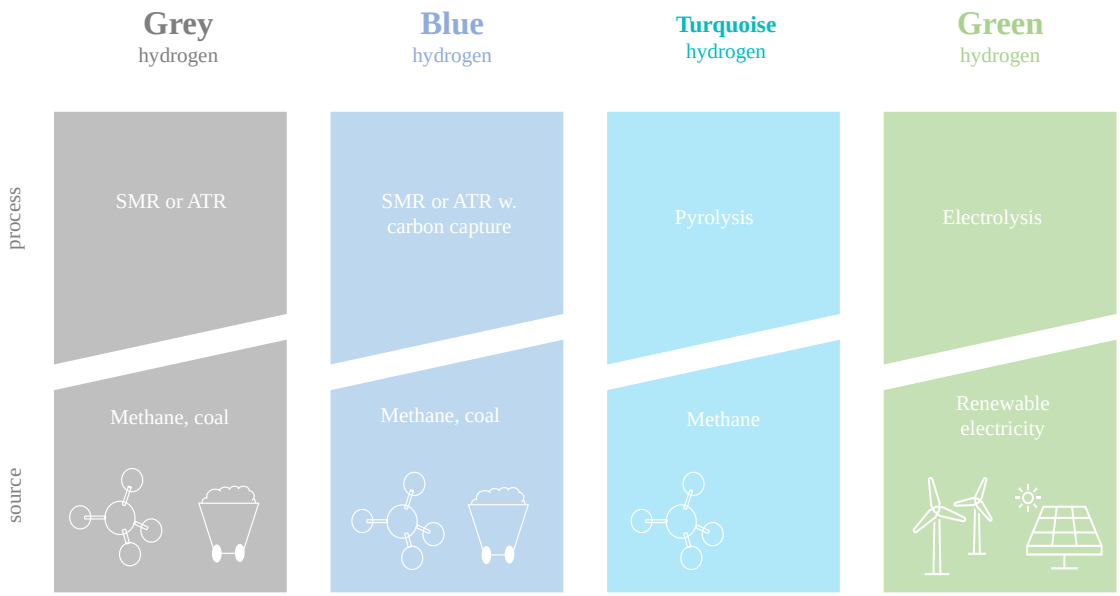

Figure 2.3: The names of hydrogen gas is connected to a colour which is related to the way of producing and the source used.

The most known electrolysis models are alcaline electrolysis (AEL) and protone exchange membrane (PEM), which have different structures and ways of operation. AEL is considered a mature technology. See figure 2.4a for visualisation of the principals of AEL. There are two electrolyser cells, both consisting of the electrolyte of normally KOH to increase conductivity. Hydrogen gas is created at the cathode when electricity is applied, while hydroxide ions are transported through the membrane towards the anode. Oxygen gas evolves at the anode after H_2O react with the transported hydroxide ions [17]. The reactions at the cathode and anode are

$$2\,\mathrm{H_2O\,(l)} + 2\,\mathrm{e^-} \rightarrow \mathrm{H_2(g)} + 2\,\mathrm{OH^-} \tag{2.3}$$

and

$$2\,\mathrm{OH^-\,(aq\cdot)} \rightarrow \frac{1}{2}\,\mathrm{O_2(g)} + 2\,\mathrm{e^-} \tag{2.4}$$

respectively.

PEM is illustrated in figure 2.4b. PEM is commercially available for low-scale production application [17]. A thin polymeric membrane leads to a proton (H^+) excluding behaviour. Water oxidation at the anode creates oxygen, electrons, and protons that travel to the anode. The electrons travel through a power source, while the protons travel through the membrane. At the anode, electrons and protons create hydrogen gas [17]

$$\mathrm{H_2O(l)} \rightarrow \frac{1}{2}\,\mathrm{O_2\,(g)} + 2\,\mathrm{H^+\,(aq\cdot)} + 2\,\mathrm{e^-} \tag{2.5}$$

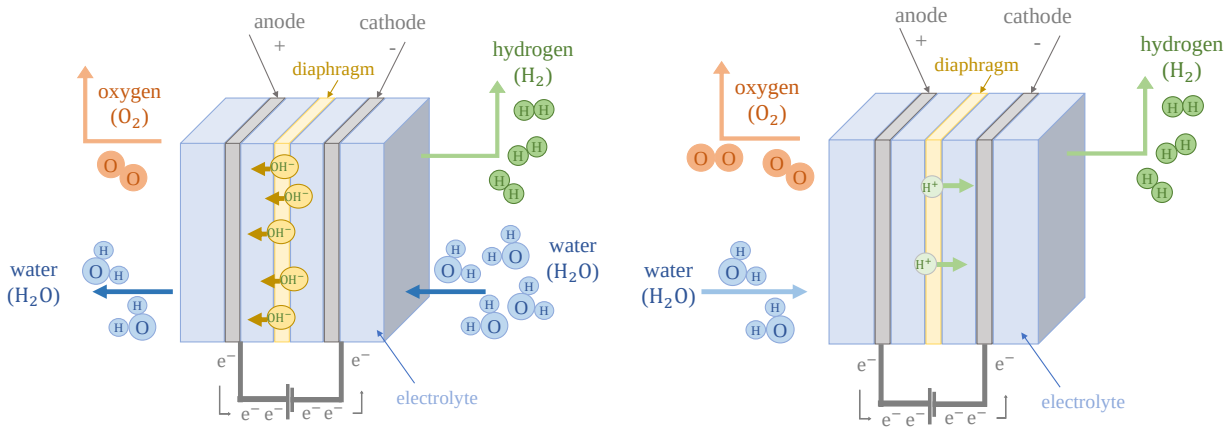

(a) Alcaline electrolysis cell (AEL).

(b) Protone exchange membrane (PEM) electrolysis cell.

Figure 2.4: Schemes of principals of alcaline and protone exchange membrane electrolysis.

and

$$2\,\mathrm{H}^+\,(\mathrm{aq}\cdot) + 2\,\mathrm{e}^- \rightarrow \mathrm{H}_2\,(\mathrm{g})\cdot \tag{2.6}$$

AEL and PEM are both ways of producing renewable hydrogen if the input energy is renewable electricity. At the same time, there are many differences in their way of operating. Furthermore, see table 2.1 for an overview of the main differences. PEM respond within milliseconds to fluctuations in input energy, while AEL responds within seconds. AEL has an operating range within 15-100 %, while PEM operate within 0-100 %. Another difference between the two is the operating pressure and the energy usage. AEL operate at 1 bar and with an energy consumption of ∼49 MWh/kg H_2, while PEM operate at 30 bar with an energy consumption of ∼59 MWh/kg H_2. AEL is a mature technology, while PEM is relatively new. Another great difference is the area demand, where AEL electrolysis require 50 % more area than PEM [3].

Table 2.1: Main differences in the operating properties of PEM and AEL technology [3].

	PEM	AEL
Operating Range	15-100 %	0-100 %
Operating pressure	1 bar	30 bar
Electrolysis efficiency	49 MWh/kg H_2	52 MWh/kg H_2

2.3 Hydrogen processing, storage and transport

The hydrogen molecule can be processed to store and transport the energy carrier more efficiently. The most common transform products are ammonia (NH_2), liquid hydrogen gas (LH_2) and compressed hydrogen gas (CH_2) [3]. NH_2 and LH_2 will be introduced in this chapter briefly, while CH_2 is introduced thoroughly due to the focus of this thesis.

2.3.1 Ammonia (NH_2)

Hydrogen can be stored chemically in NH_2. NH_2 is already a known product in the industry, and it is mainly used as an artificial fertiliser or as fuel in an engine with no emission of greenhouse gases. It has only 40% of the volumetric energy density of diesel, but NH_2 has double the energy density of LH_2. Production of ammonia is by the Haber-Bosh technology, which combines Nitrogen gas and Hydrogen gas to NH_2. This technology uses less than 40% of the energy needed to create LH_2 [3].

2.3.2 Liquid hydrogen (LH_2)

Liquid hydrogen has the advantage of having a high energy density compared to, e.g. compressed hydrogen. A combination of compression and cooling is needed in order to process LH_2, and cryogenic technology is needed for transport and storage. By 2022, large-scale hydrogen storage and transport in liquid form still face many challenges, significantly within storage and transportation [19]. Due to the low liquefication temperature of 20° over the absolute zero, LH_2 has significant boil-off losses when handled, and ships are the only option for transport so far. On the other hand, is LH_2 a concentrated form of hydrogen. In comparison with compressed hydrogen, it has an energy density of 2.8 kWh/L, which is three times the energy density of CH_2 [3].

2.3.3 Compressed hydrogen gas (CH_2)

Hydrogen gas has a low energy density, but it is increased when higher pressure is applied to the gas. Compression of hydrogen demand only 6 % of the energy content to increase the pressure from 30 bar to 875 bar. There is already exciting infrastructure for production, compression, transportation and storage of CH_2 [20]. The compression process can be adiabatic, isothermal or multistage. Adiabatic compression has no heat transfer with the surroundings, and the work, W_{ad} is expressed as

$$W_{ad} = \frac{\gamma}{\gamma - 1} p_0 \, V_0 \, [\frac{p}{p_0}^{\frac{\gamma-1}{\gamma}} - 1], \tag{2.7}$$

where γ is the ratio of specific heats, p is the resulting pressure after compression and p_0 and V_0 is the initial pressure and volume. Isothermal compression is a slow compression with a constant temperature and the expression for the work, W_{iso}, is

$$W_{iso} = p_0 \, V_0 \, \ln(\frac{p}{p_0}). \tag{2.8}$$

Multistage compression is a possible way to compress hydrogen, which is a limit between adiabatic and isothermal compression [21]. Application of the compression in many steps with cooling the gas results in energy use between the adiabatic and isothermal compression. The figure 2.5 shows the different energy usage for initial pressure of both 1 and 30 bar. The work done by a multistage compressor, W_{multi} can therefore be expressed as

$$W_{multi} = [W_{iso} + W_{ad}]/2, \tag{2.9}$$

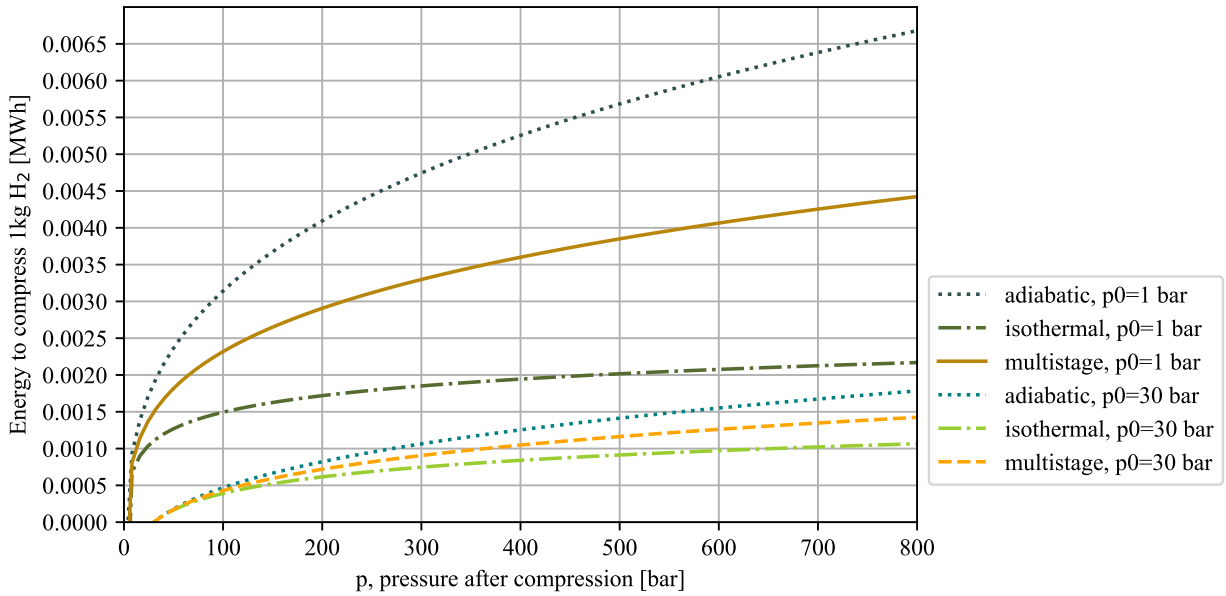

Figure 2.5: Energy consumption in adiabatic, isothermal and multistage compression for an initial pressure of both 1 bar and 30 bar.

where W_{iso} is the work of the isothermal compressor and the W_{ad} is the work of the adiabatic compressor according to chosen resulting pressure and initial pressure.

When variable renewable energy is the power source in hydrogen production, storing the gas to have a reliable hydrogen source is favourable. Compressed hydrogen storage is the most established technology, which involves the physical storage of compressed hydrogen gas in high-pressure vessels. 700 bar can be the storage pressure of hydrogen, but for large scale storage, 350 bars is the optimal pressure of the technology of 2022. Compressed hydrogen can also be stored underground in large scale cavities. Salt caverns are the most promising large scale storage solution with low permeability, ensuring minimal loss. Salt caverns can store hydrogen up to 180 bar if there are rapid storage and release rates [22]. There is also minimal geological contamination from surroundings [23]. Section 4 present a further state of the art discussion and comparison of compressed hydrogen storage options in the North Sea.

When converting from mass to volume at a given pressure can hydrogen gas be assumed an ideal gas, and the following formula for the resulting volume, V_{H_2}, is used

$$V_{H_2} = \frac{m_{H_2}}{P_{H_2}} * R * T \tag{2.10}$$

where m_{H_2} is the mass of the hydrogen gas, P_{H_2} is the pressure, R is the universal gas constant, and T is the temperature.

If a gas storage solutions potential is given in Power (W), the resulting mass of the working gas can be calculated as follows

$$m_{workinggas} = \frac{cavernCapacity}{LHV_{workinggas}}, \tag{2.11}$$

where $cavernCapacity$ is the energy amount which can be stored in the storage solution, and the $LHV_{workinggas}$ is the lower heating value of the gas of consideration [24].

2.3.4 Hydrogen transport in pipeline

Transportation of CH_2 is either by pipelines, ships or trucks, depending on the transportation route. There is a great network of pipelines transporting natural gas from the oil and gas industry all around Europe. See figure 2.6 for an overview. There is a research group at Sintef, a Norwegian independent research organisation, which study whether the existing pipelines produced to transport natural gas are applicable for Hydrogen transport and is called HyLINE [25]. If possible, the transportation cost of hydrogen gas could be reduced considerably.

When gas is transported in a pipeline, energy loss occurs in the form of pressure loss. This is due to the major head loss from friction forces from the irregularities in the pipeline. The Bernoulli equation can express the fluid friction between two points in a pipeline,

$$\frac{v_1^2}{2g} + \frac{p_1}{\rho g} + z_1 = \frac{v_2^2}{2g} + \frac{p_2}{\rho g} + z_2 + h_L, \tag{2.12}$$

where v is the average velocity, g is the gravitational acceleration, p is the pressure, z is the elevation of the pipe, ρ is the fluid density, and h_L is the major head loss between 1 and 2. The denotation 1 and 2 refers to the two positions at the pipe. When there is no change in pipeline diameter, the velocity terms cancel due to no change in the velocity. When the elevation of the pipe is the same at 1 and 2, z cancel as well [26].

The Darcy-Weisbach equation is used when calculating pressure drop, ΔP, in a pipeline. It is initially meant for incompressible fluid flows and does not account for gas compressibility. At the same time, it can be used if the resulting pressure drop is below 10 % of the inlet pressure [27]. This is due to the infinitesimal change in the density due to the slight change in pressure. Julius Weisbach proposed the following equation for friction head loss in 1845

$$h_l = \frac{fL}{D}\frac{v^2}{2g}, \tag{2.13}$$

where f is the friction factor, L is the pipe length, D is the diameter, v is the velocity, and g is the gravitational acceleration. Major and minor head loss is in a pipe, where minor head loss is due to elbows and other fittings. h_l only considers the major head loss due to viscosity and wall friction. In order to calculate the friction factor f, the Reynolds number Re needs to be calculated with the following formula

$$Re = \frac{vD}{\nu}, \tag{2.14}$$

where v is the velocity, D is the pipe inner diameter and ν is the kinematic viscosity. The flow is determined either turbulent or laminar from the Re, the Reynolds Number. The flow is turbulent if $Re > 4000$, and laminar if $Re < 2000$. The in between limit is called critical flow. The friction factor f has two expressions depending on the Reynolds number [26]. If the flow is laminar, is

$$f = \frac{64}{Re}. \tag{2.15}$$

If the flow is turbulent, the formula for the friction factor is the following.

$$\frac{1}{\sqrt{f}} = -2\log(\frac{\epsilon}{3.7} + \frac{2.51}{Re\sqrt{f}}), \tag{2.16}$$

which is called the Colebrook equation and is valid if the flow has a Reynolds number between $4000 < Re < 80,000$. The resulting pressure drop is calculated by multiplying the head loss in the following way

$$\Delta P = h_L * \rho_p * g, \tag{2.17}$$

where ρ_p is the density of the gas at pressure p, and g is the gravitational force.

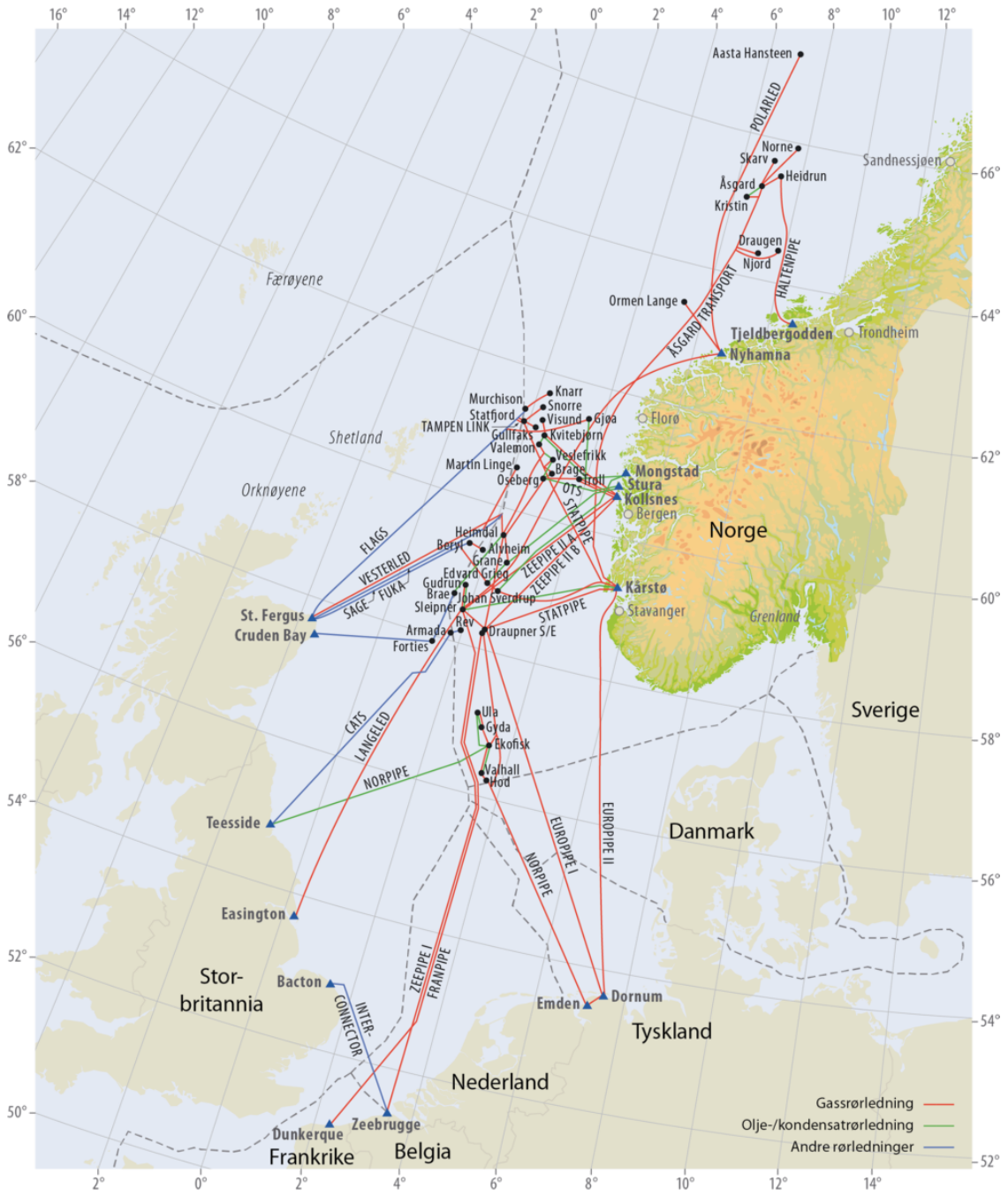

Figure 2.6: The existing network of pipelines intentionally made for natural gas and oil [28]. Red pipes is for gas, green is for oil and blue is for other. A researchers group at Sintef, HyLINE, is studying the potential of utilising the already existing pipelines for hydrogen transport [25].

3 Method

3.1 Offshore wind to hydrogen systems

The python script used to calculate the results is developed in combination with the project thesis written in 2021, named *Case study on hydrogen production from offshore wind power*. The script from the project thesis lays the basis for this thesis by calculating the hydrogen output from an offshore wind power plant. The further development of the script in this master thesis includes a storage solution, and the calculation method is further described in section 3.2. The python script for storage calculation is in the appendix, 9.

To collect and transform weather data from a chosen location to power capacity data is `renewables.ninja` used. The weather data in `renewables.ninja` is from NASA MERRA reanalysis or CM-SAF's SARH dataset [29]. The main input parameter is the wind turbine model. The Virtual Wind Farm model converts weather data to power curves. Other sources describe the model in detail [30]. The output is data with hourly generated power in one year.

The method from the PhD of Magnus Korpås lays the basis of the approach to calculate the amount of produced hydrogen from an offshore wind power plant [31]. It uses linear conversion, which is a simplification of detailed calculations. To calculate between energy sources is the following method applied.

When an offshore wind farm generates electricity, it is first converted to direct current (DC) from alternating current (AC) and further transmitted through cable before reaching the location of utilisation. In this case, the goal is an offshore electrolyser platform, and all of the power produced at the wind power plant is supplied to the electrolyser. The power grid is integrated later, in the method of section 3.3. To calculate losses between the wind turbines and the electrolyser is, the following formula used

$$E_{EL} = E_{wind} * P * (1 - \eta_{cable+converter}), \tag{3.1}$$

where E_{wind} is the power created by the wind farm that hour in decimal of total capacity, P is the maximum power, $\eta_{cable+conv}$ is the loss in the cable transmitting the power from the wind power plant with converter energy loss added. The electrolyser receives the power from the converter and creates hydrogen. The amount of created hydrogen is expressed by the following equation,

$$m_{H_2} = \frac{E_{EL}}{\eta_{PEM}}, \tag{3.2}$$

where E_{EL} is the power supplied to the electrolyser, η_{PEM} is the efficiency of the electrolyser given in MWh/kgH_2. The hydrogen gas needs to be compressed before it is transported through a pipeline. The compression energy demand is expressed as

$$E_{comp} = m_{H_2} * \eta_{compr}, \tag{3.3}$$

where m_{H_2} is the amount of kg hydrogen which is compressed and η_{compr} is the efficiency of the compressor given in $MWh/kg\,H_2$. In this thesis, the compressor is a multistage compressor, and the η_{compr} can be

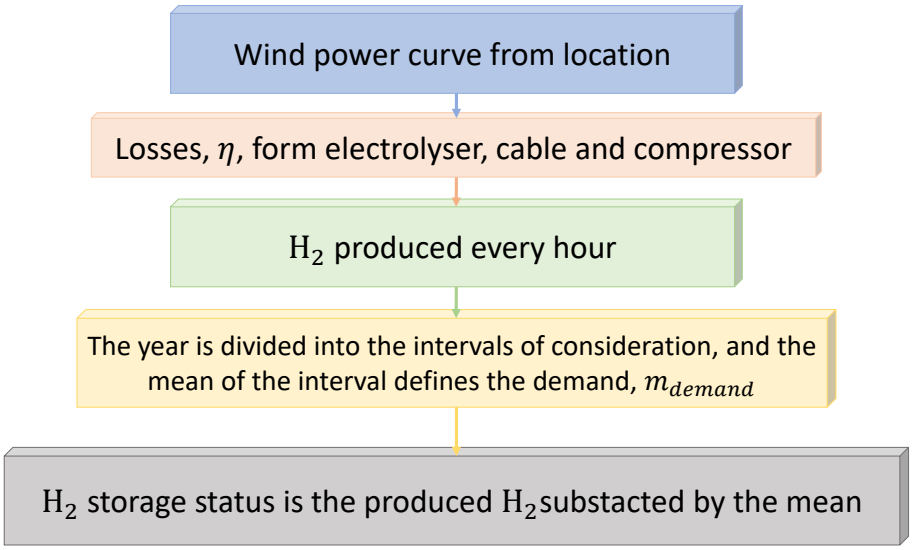

Figure 3.1: Flow chart of the python script used to calculate the hydrogen storage status. The interval for constant delivery is both yearly, monthly, and 9.125 days, 5 days and 1 day constant interval.

calculated as follows

$$\eta_{compr} = [\eta_{iso} + \eta_{ad}]/2 \tag{3.4}$$

where $\eta_{isothermal}$ is the efficiency of the isothermal compressor and the $\eta_{adiabatic}$ is the efficiency of the adiabatic compressor at according to chosen resulting pressure and initial pressure.

3.2 Storage integration

Investigation of a hydrogen storage facility's sizing requires the establishment of the necessary hydrogen demand. The method of this thesis defines the hydrogen demand to be the same as the mean hydrogen produced in an interval. Hydrogen gas is either added or withdrawn from the storage, depending on the amount of produced hydrogen. The amount of hydrogen gas added or withdrawn from the storage is

$$m_{H_2,storage} = m_{H_2,produced} - m_{H_2,demand}, \tag{3.5}$$

where $m_{H_2,produced}$ is the amount of produced hydrogen gas that hour, $m_{H_2,demand}$ is the constant hydrogen demand delivered to the end-user and $m_{H_2,storage}$ is the amount of hydrogen gas added or withdrawn from the storage, depending on the sign. If the sign is negative, the hydrogen gas is withdrawn from the storage. If the sign is positive, the amount of hydrogen is added to the storage. Figure 3.1 shows a flow chart for the python script used to calculate the hydrogen storage demand for cases with varying intervals for continuous delivery.

To observe the difference in the hydrogen storage demand, the intervals for continuous delivery are varied. One of the cases had continuous delivery the whole year, called a yearly interval. The other interval divisions were monthly interval, 9.125 days interval, 5 days interval and 1 day interval. In that distinct interval was a continuous delivery to shore. The compression of the hydrogen for transport and storage is

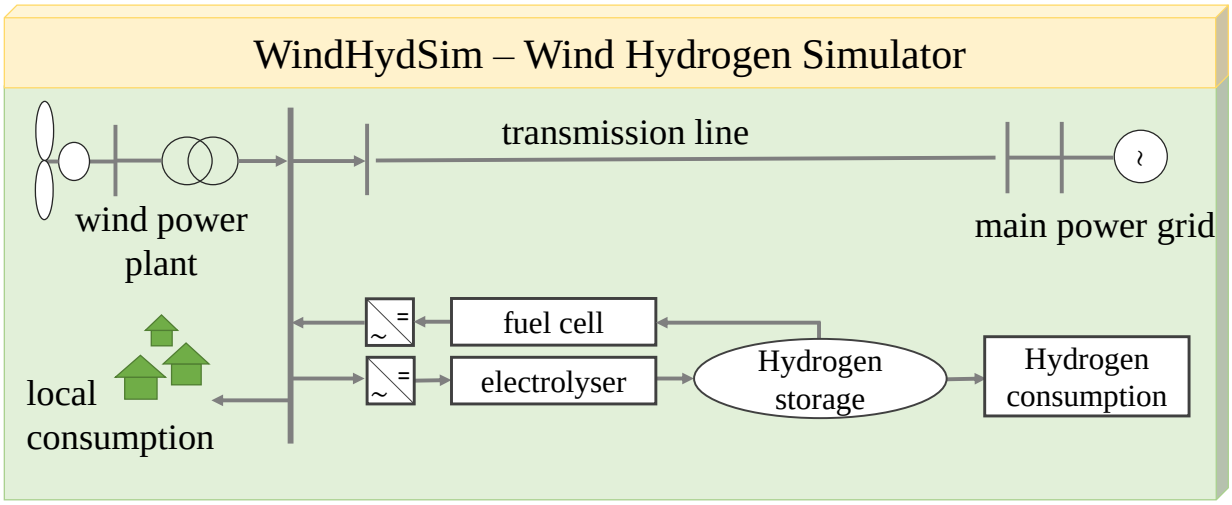

Figure 3.2: Schematic illustration of the all of the possible components in the wind to hydrogen system in *Windhydsim*. It integrates a wind power plant, local electrical load, fuel cell, electrolyser, hydrogen tank, local hydrogen load, electrical power cable and the grid. The figure is inspired by a figure in [32].

not included in this model to have the flexibility of choosing the storage solution later.

3.3 Grid integration

To calculate the model in combination with grid integration, is the program *Windhydsim* used. Windhydsim is a Matlab/Excel based program written by Magnus Korpås in association with his the PhD [31]. It simulates a wind-hydrogen energy system. The program goal is to get an overall objective of the sizing of different components to predict the average performance of the system as a whole. The basis is an hour to hour simulation where input parameters are wind power data, electrolyser efficiency, hydrogen storage capacity, grid import and export and electrical load data. The model calculates the energy and hydrogen balance for each time step [32]. Figure 3.2 shows a schematic illustration of the complete wind to hydrogen system with the wind power plant, a local load, fuel cell, electrolyser, hydrogen storage, hydrogen load, electrical power cable and grid connection in WindHydSim.

Figure 3.3 shows two flowcharts of the *Windhydsim* Matlab program. Figure 3.3a shows the main flow chart, while figure 3.3b shows the flowchart of the belonging function *simloop*. First, the main flow chart, being the Windhydsim program, reads the excel file and reads the component parameters, simulation parameters, needed text files, and time series. After that, it simulates the time steps using *simloop* and calculates the main results with the results from the simloop iteration. Then it writes all the time series and main results to excel and exits. The function simloop sets the storage level and reads the input data. Then it calculates the energy and hydrogen balance for the chosen strategy in N time steps. After that, it returns the

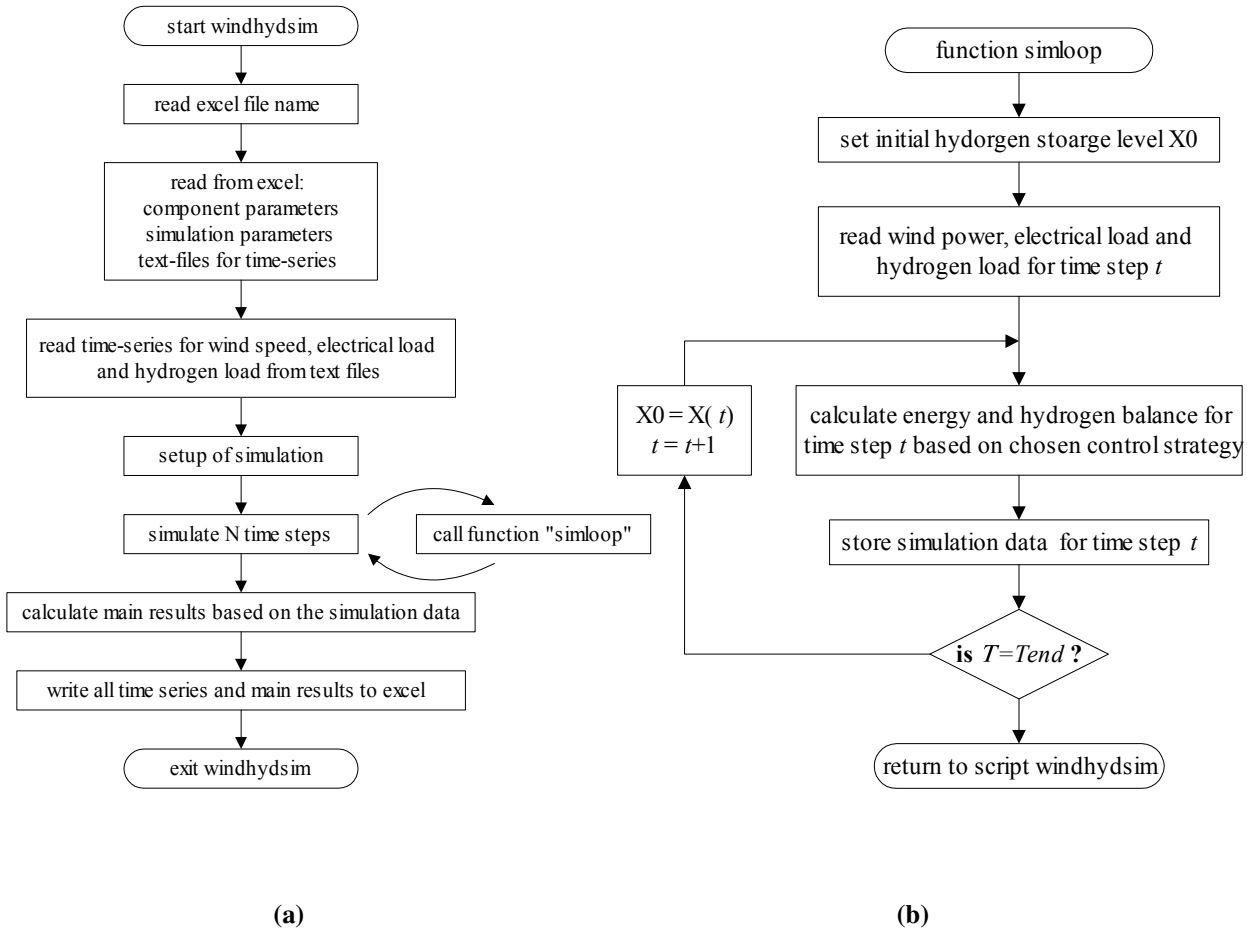

Figure 3.3: (a): Flow chart of the Matlab program Windhydsim, which is used to calculate the simulate wind to hydrogen systems [32]
(b): Flow chart of the Matlab program simloop which is used to calculate the energy and hydrogen balance in each time step [32].

results to the main function [32].

3.3.1 Control strategy

There are several control strategy opportunities in the Windhydsim program. The strategy used in the models of this thesis is *Wind power primarily for the hydrogen filling station*, which is strategy number two. Figure 3.4 shows the included components in the chosen control strategy. The control strategy has set the electrolyser to produce hydrogen when the wind power exceeds zero and produces hydrogen with power from the grid electricity if the hydrogen level reaches the supply security limit. Firstly, the main goal is to deliver the hydrogen demand and then refill the hydrogen storage if possible. Export of power happens when the hydrogen demand is supplied and the hydrogen storage is full. Power is imported from the grid if the generated wind power is not enough to supply the electrolyser to produce the hydrogen demand and the

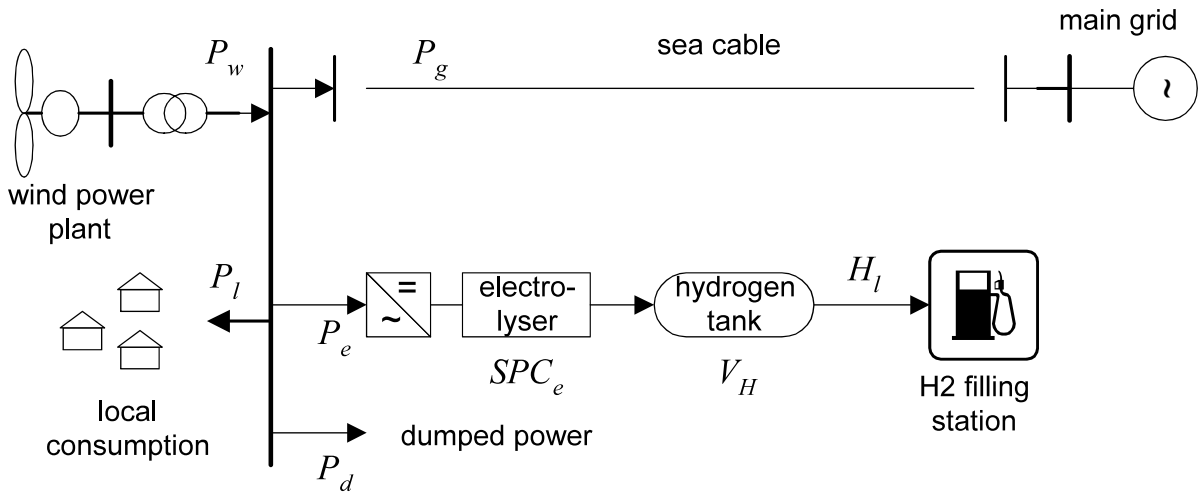

Figure 3.4: Illustration of the included component of the control strategy *Wind power primarily for the hydrogen filling station*. In the model of this thesis is the local consumption set to zero [32].

storage is empty. The control strategy has no fuel cell integrated, and all of the models in this thesis have a local power demand set to zero [32].

Figure 3.5 shows the flow chart of the Matlab code of control strategy number two, *Wind power primarily for the hydrogen filling station*. It shows how the energy from the sources is divided and distributed among the products being the hydrogen and the export power [32].

3.3.2 Storage size variation

Variations of the total hydrogen storage size are applied to study the amount of grid transmission. The storage size varies as a percentage of the total storage demand for continuous delivery to shore in the interval. The total storage demand for continuous delivery is the storage size required to deliver constant hydrogen to the end-user in the investigation interval. It is calculated by the method described in section 3.2. The storage size is decreased to 50 % and 10 % of the initial 100 % storage demand. The new size of the storage capacity is integrated into the Matlab model by changing the input value *hydrogen storage capacity* to the new size by multiplying the original total storage capacity by a factor of 0.5 or 0.1 for a 50 % or 10 % storage capacity, respectively. Section 5.3.1 further presents the combinations of the interval divisions, wind power capacities and storage capacities.

3.4 Storage capacity calculation

The potential for hydrogen storage in the salt cavern is found in the article written by Caglayan et al. [24]. The potential is presented in TWh, which is transformed to the potential mass of working gas mass by using equation 2.11. The method used to investigate the potential of utilising the salt cavern potential for hydrogen storage is shown in figure 3.6. The method is first to calculate the amount of hydrogen gas, $m_{workinggas,cavern}$, which can be stored in the salt cavern. Then, a wind to hydrogen model is created, using

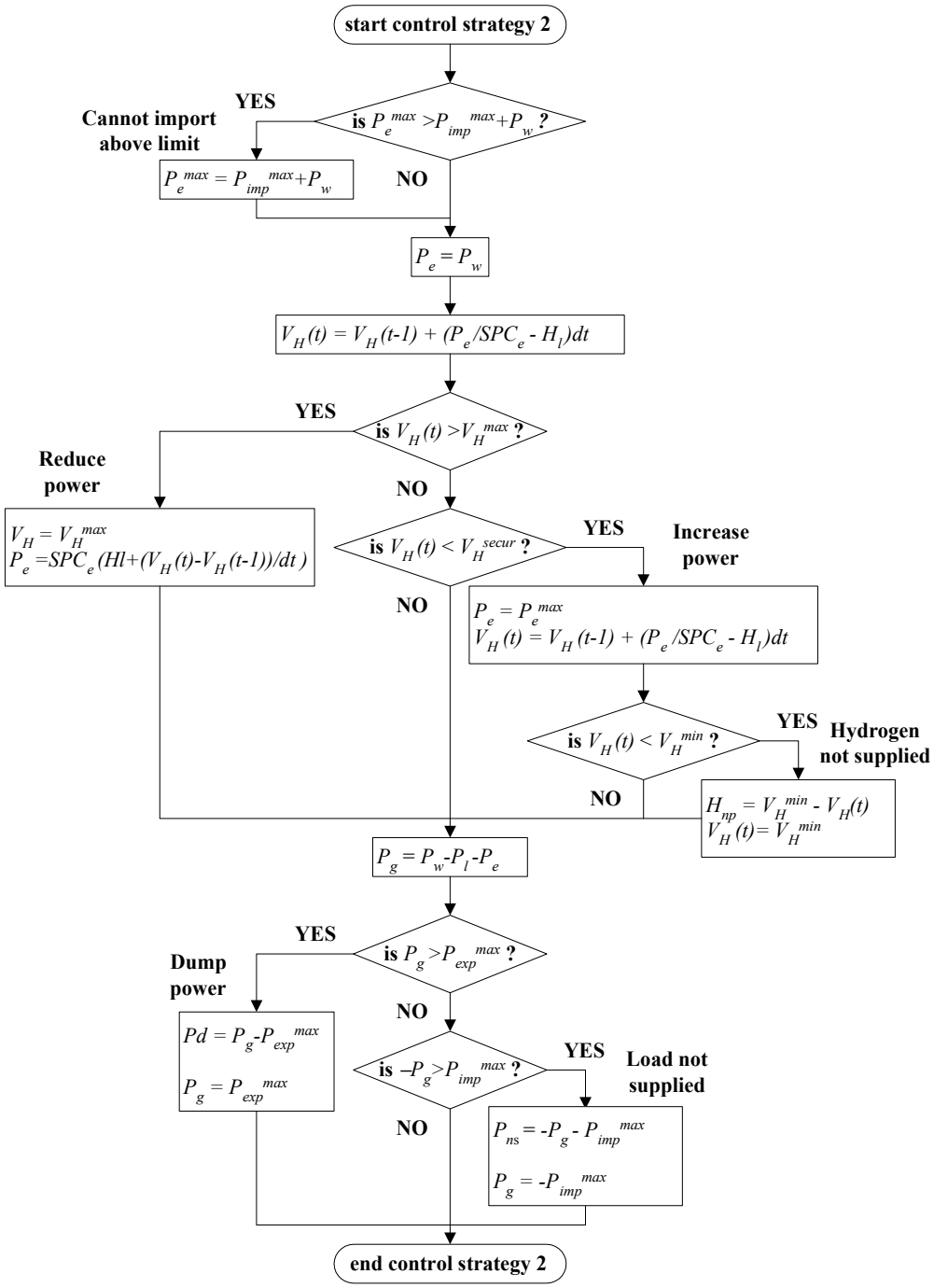

Figure 3.5: Flow chart of the Matlab code of the control strategy 2, *Wind power primarily for the hydrogen filling station*. P_w is the wind power, P_g is the grid power, P_l is the local consumption, P_e is the electrolyser power, P_d is the dumped power, P_{ns} is the local consumption not supplied, dt is the simulation time step, $V_H(t)$ is the hydrogen storage volume in present time step, $V_H(t-l)$ is the storage volume of the previous time step, SPC_e is the specific power consumption of electrolyser, ${P_e}^{max}$ is the maximum electrolyser power, P_f^{max} is the maximum fuel cell power, ${P_{imp}}^{max}$ is the maximum import power from grid, ${P_{exp}}^{max}$ is the maximum power export to grid, ${V_H}^{max}$ is the maximum hydrogen storage volume and ${V_H}^{min}$ is the minimum hydrogen storage volume [32].

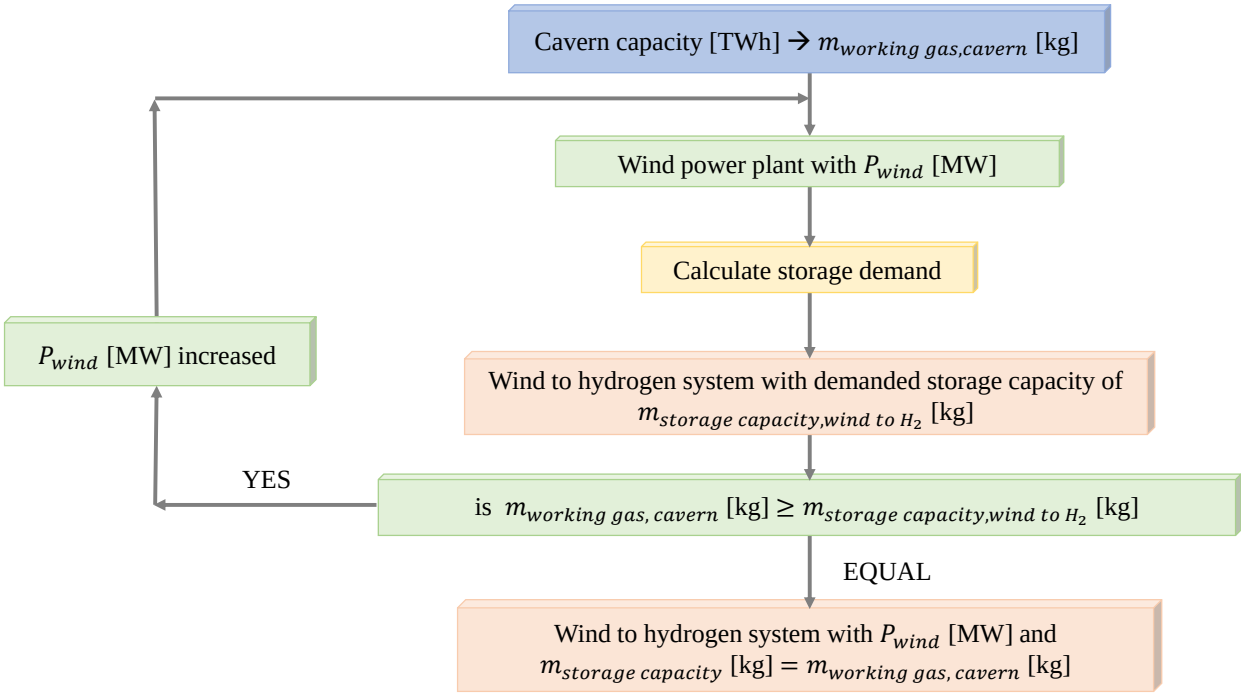

Figure 3.6: Visualisation of the method of calculating the size of a wind to hydrogen power plant which utilises all of the storage potential in the salt caverns estimated to be located in the Norwegian North Sea territory.

the method described from section 3.1, and includes a storage solution with the method shown in section 3.2. The wind to hydrogen system, which is also used in the salt cavern storage capacity calculations, is further described in section 5. The model has a given P_{wind} in the MW order and uses the method shown in figure 3.1 to calculate the hydrogen storage demand, $m_{storagecapacity,windtoH_2}$. This demand is compared to the $m_{workinggas,cavern}$. If there is remaining storage capacity, the power of the wind power plant is increased, and the salt cavern storage potential is again compared to the storage demand. If they are the same, the size of the wind to hydrogen system, which utilises all of the storage capacity, is found. The model also delivers a continuous hydrogen delivery to shore every hour for the whole year.

4 Hydrogen storage options in the North Sea

This chapter presents status of the hydrogen storage technology, and the assumed most promising storage technologies for hydrogen storage in the North Sea.

Hydrogen is often considered one of the solutions for making variable renewable energy more reliable due to the energy carrier characteristics of the element. In order to be a reliable energy carrier with easy access in high demand periods, it needs to be stored. As wind power technology transitions offshore, seasonal energy storage at the ocean is needed. Subsea storage technology for natural gas in the petroleum industry has developed in the past decades. The petroleum technology has distributed and controlled pressurised oil and gas up to 700 bar, and a transition into 100 % hydrogen could be within reach [33]. Still, there are some critical differences between hydrogen and natural gas storage. Some materials can suffer from embrittlement in contact with hydrogen, which can cause material failure. Another difference with natural gas storage is the size of the molecule. Hydrogen can leak through valves and pipeline sections meant for natural gas transportation and storage [34].

Liquid hydrogen is dense but has a boiling point of 20 degrees over absolute zero. It is, therefore, technically challenging and energy-intensive to store liquid hydrogen in a large scale with the technology of 2022. Ammonia is another promising offshore processing and storing alternative. It is because ammonia is liquefied at 7.5 bar at room temperature, which is the pressure achieved at 75-meter depth [3]. However, compressed hydrogen is often considered for large scale storage of hydrogen and is the most established storage technology [23]. There are two main methods for storing compressed hydrogen: storage vessels and geological storage. There are also many other ways of storing the element, but due to the focus on subsea storage, these two technologies assumed the most relevant [34].

4.1 Geological underground hydrogen storage

The oil and gas industry has practised geological storage of natural gas for decades, and the technology is possible to transfer into hydrogen storage due to cavern design, construction and depletion similarities [24]. Salt caverns, depleted oil and gas reservoirs and aquifers are the main types of underground storage technologies which can be applicable for underground hydrogen storage [22].

4.1.1 Salt cavern storage

Salt caverns are considered the most promising low-cost alternative for large scale hydrogen storage, with an estimated price of 0.0205 EUR/kWh [35]. Salt caverns also have low safety costs due to rock salt's low hydrogen permeability, leading to high sealing capacity. The only constraint is, therefore, the size of the cavern itself. Another advantage of salt caverns is the low cushion gas requirements of 33 % and storing pressures up to 200 bar [23].Cushion gas is the base gas required for operation. The flexible operation with high injection and with drawl rates makes this storage technology suitable for large storage of hydrogen from variable renewable energy sources [22].

Hydrogen has been stored in salt caverns for many years already. One salt cavern storage facility has operated since 1972 in Teesside, UK. It stores 25 GWh of hydrogen at 45 bars in three separate salt caverns.

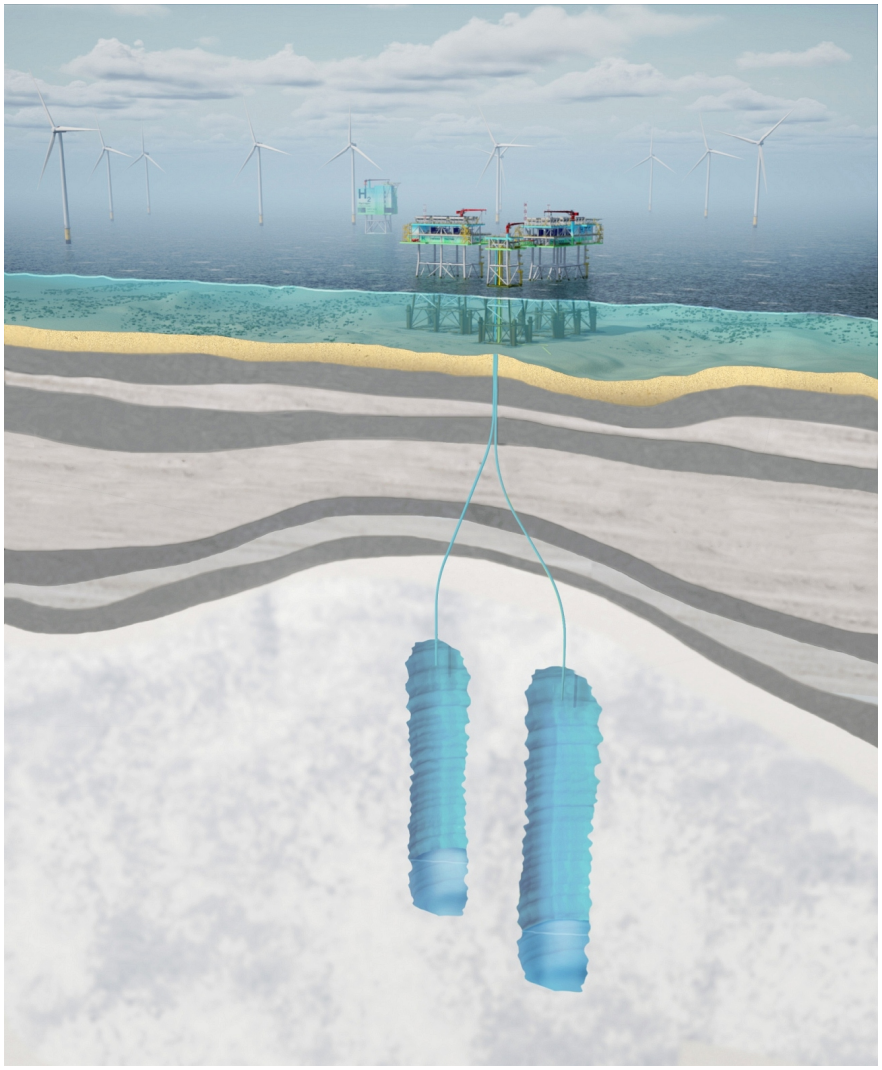

Figure 4.1: Visualisation of the hydrogen processing, compression and salt cavern storage from Tractebel. The company will store hydrogen at 180 bar in an underground salt cavern in the North Sea [36].

Texas has salt cavern storage facilities in Clemens Dome, Moss Bluff and Spindletop. The one in Clemens Dome has operated since 1983 with a capacity of 92 GWh and storage pressure between 70 and 135 bar. Moss Bluff and Spindletop have capacities of 120 GWh, respectively [23]. There are no known operating subsea salt caverns for offshore hydrogen storage.

The engineering unit of global energy giant Engie, the Belgian Tractebel, will be the first to use offshore underground salt caverns to store gaseous hydrogen. Their facility will be able to store 1.2 million cubic metres of hydrogen in underground salt caverns and will therefore be a "hydrogen hub" at sea. The company will store hydrogen at 180 bar with a capacity of hydrogen produced by 2 GW offshore wind but will be scalable both up and down. See figure 4.1 for a visualisation of the subsea salt cavern storage technology from Tractebel [36].

The North Sea salt caverns are well suited for hydrogen storage due to the geology [36]. Figure 4.2 shows the storing potential in The North Sea.

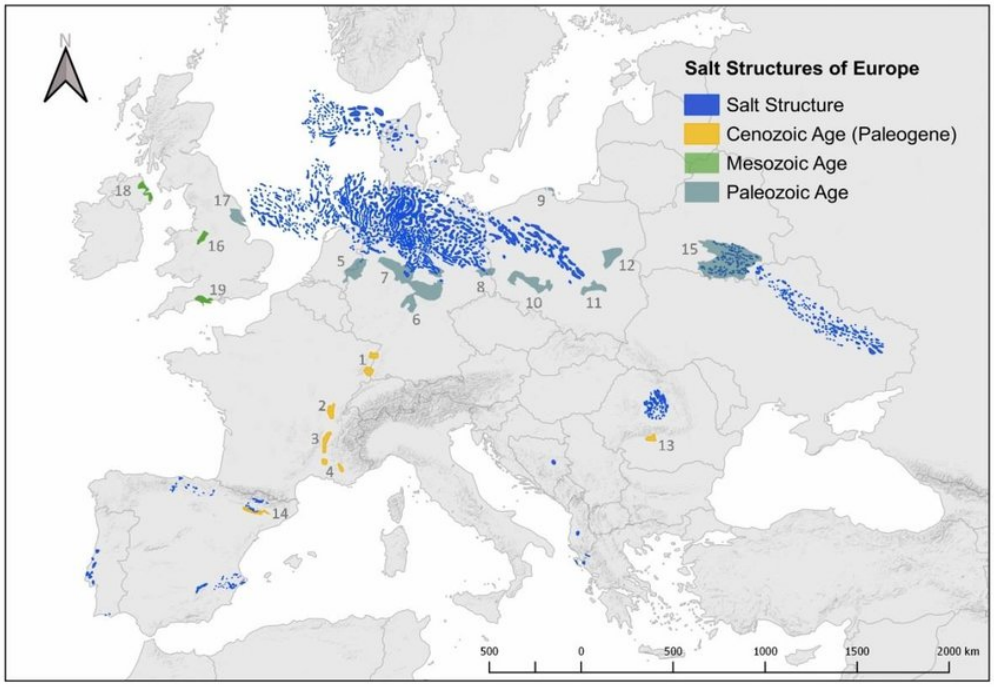

Figure 4.2: Map of potential salt deposits in Europe [24].

4.2 Storage vessels

The industry has broad experience storing and transporting gas in pressure vessels, ranging from small bottles to massive storage tanks [23]. Choosing materials that minimise the risk of embrittlement caused by hydrogen absorption and dissociation when handling hydrogen is crucial. Embrittlement reduces the strength and durability of the material. Materials like authentic stainless steel, aluminium and copper alloys are known for resisting the effects of hydrogen absorption and dissociation. The sizeable stationary storage vessels can store hydrogen from 100 to 825 bars [23]. The pressure difference depends on the material and the type of vessel [8]. The cost of storage pressure vessels is estimated to be 13 EUR/kWh [8]. A though review of the characteristics of the different types of storage vessels can be found elsewhere [23].

4.2.1 Sub sea tanks

One of the most significant expenses when establishing hydrogen production offshore is the platform cost. In order to save area and, therefore, the cost when producing hydrogen offshore, the company TechnipFMC investigates the potential of storing hydrogen in subsea tanks. The name of the project is and has the leading industrial partners being Vattenfall, Repsol, Sintef, ABB, NEL, DNV, UMOE and Slåttland [37]. The pressure tanks store hydrogen in 300-350 bars. In 2024 is, a small scale land-based pilot of the Deep Purple project planned to be operating, and Innovation Norway is founding the project [38]. The project has received funding from the Research Council of Norway [39]. See figure 4.3 for a technical sketch of the Deep Purple project.

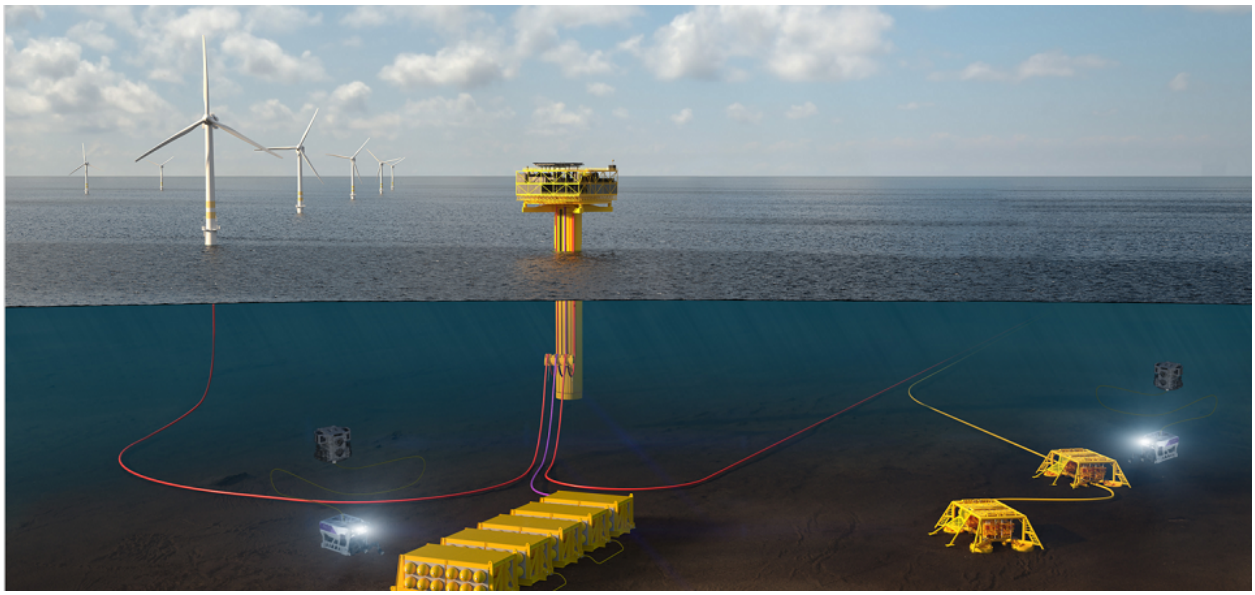

Figure 4.3: Sketch of the Deep Purple project of TechnipFMC [38]. The project plan is to store hydrogen subsea in pressure vessels.

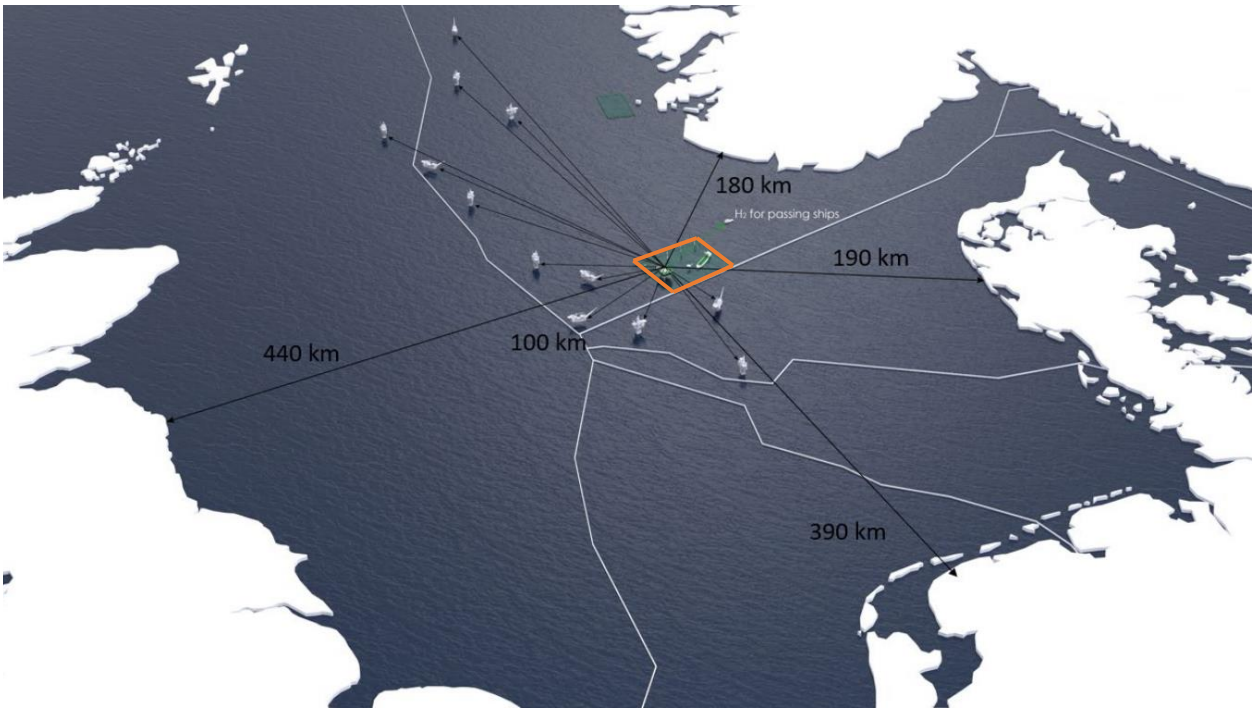

Figure 5.1: Location of the Southern North Sea II in the Norwegian North Sea territory and the distances to nearby shore [3].

5 System description

5.1 Offshore wind electricity production

The chosen area of consideration for the offshore wind farm is Southern North Sea II (SNII). It is placed on N 56° $78.8990'$ E 4° $89.8230'$, which is on the Norwegian side of the border to the Danish territory. It has a total area of 2,591 km^2. Figure 5.1 shows the location of the area in the North Sea and the distances to shore. The location makes international connections possible. In February 2022, the Norwegian Government announced the plan to construct a 1500 MW offshore wind power plant [4]. Therefore SNII is a natural area to consider for offshore wind power production.

The weather in the North Sea is rough and is one of the best in Europe when considering offshore wind power spots. It has a slight difference from the weather nearer Netherlands and UK, which makes it a good spot for potentially connecting to the international power grid [3]. The distance from the Norwegian and Danish shores is approximately 200 km and is, therefore, the chosen distance for the ending point for the hydrogen gas in this case study. The depth is 60 meters, making it possible to install bottom-mounted jacket structure turbines. The chosen turbine for this case is the *MHI Vestas Offshore V164-10.0MW* which has a capacity of 10 MW [40]. Seagreen offshore wind park is installing the MHI Vestas v164 in 2022 with a jacket structure foundation. The Scottish North Sea is the chosen area for the wind power plant in the Seagreen project, where the depth is 40-60 meters [41]. The turbine has a hub height of 105 m, a diameter of 164 m, and a swept area of $21,124$ m^2 [40]. The diameter of the turbine's rotor is the same height as

twice the height of the spire in the Nidaros Cathedral in Trondheim.

The weather data used to model the power generation for this thesis's modelled wind power plant is only available from 2019. 2019 is considered a mean year in between others, and the storage level is therefore not at zero at the beginning of the year. The same is at the end of the year, when the storage level is above zero.

AC is generated when the wind turbines operate at sea. Cables transmit the electricity through an inter-array grid connected to a converter placed on a platform offshore. The converter converts AC to DC, which is suitable for both transport to shore and hydrogen production in an electrolyser. After the conversion, the electricity transmits through high voltage direct current (HVDC) cable to the offshore hydrogen production platform. Later, is the model extended with a grid connection, and the power can therefore later be transmitted to the power grid in addition to supplying the electrolyser. The loss of voltage between the electricity generator, after transmitting through the cable and converted is $\eta_{cable+conv}$ which is approximated to 3 $\%$ [42].

An overview of the constants needed for the calculation of the produced electricity at the offshore wind farm is found in table 5.1. The total capacity, P, is inspired by a similar case in the Greenstat report [3] and the turbine model is inspired by the Seagreen project with the same turbine to be established [41].

Table 5.1: Input numbers and component info in order to calculate the supplied power in the electrolyser.

Parameter	value
Loc. SNII	N 56° 78.8990′ E 4° 89.8230′
Turbine model	MHI Vestas Offshore V164-10.0MW
Hub height	105 m
P_{tot}	1400 MW
$\eta_{cable+conv}$	3 %
$\eta_{cable\,shore}$	2 %

5.2 Hydrogen production and compression technology

The chosen electrolyser for this model is PEM due to the operating range from 0 to 100 %, and has a reaction time of milliseconds. It makes the PEM to rapidly react to changes in power input. That is an excellent property when the power input is variable renewable energy with fluctuating power generation. The operating pressure of 30 bar is also an advantage with the PEM electrolyser due to a decrease in energy consumption when compressing the gas. PEM has never been established on a large scale before. Since the electrolysers are module-based, is the establishment of a large scale PEM electrolyser considered possible.

Seawater is the H_2O source of the electrolyser when the electrolyser is placed on a platform out in the ocean. The electrolyser demand freshwater, and desalination of the seawater is therefore necessary. The energy consumption of this process is approximated to 3 kWh/tons$_{H_2O}$, and approximately 100 litres per kg produced hydrogen [3].

Compression is needed to transport the H_2 gas in an energy-efficient way. The resultant hydrogen gas has to have a pressure of 100 bar at the goal location. The compression method is multistage compression,

which is a mean of adiabatic and isothermal compression. The values needed to calculate the amount of hydrogen gas produced, the energy needed to compress the gas and the storage conversion from power to the mass of hydrogen is listed in table 5.2. The η_{PEM} is the efficiency of the PEM electrolyser, which is 0.052 MWh/ kg H_2, p_0 is the initial pressure of the gas, T is the temperature, γ is the specific heat of H_2 gas, M is the molar mass of H_2 gas and R is the universal gas constant. LHV_{H_2} is the lower heating value of hydrogen, $p_{saltCavern}$ is the storage pressure in salt caverns, $p_{pressureVessel}$ is the storage pressure in pressure vessels, and $p_{pipelineTransportation}$ are the pressure in pipeline transport of hydrogen. Both the η_{PEM} and T are inspired by the values of the same components in the report by Sæbø et al. [3].

Table 5.2: Input numbers to calculate the amount of hydrogen gas produced, the compression energy needed, and storage conversion from mass to volume of the hydrogen gas.

Parameter	value	application
η_{PEM}	0.052 MWh/kgH_2	kg calc.
p_0	30 bar	E_{compr} calc.
T	10° C/ 283K	E_{compr} calc.
γ	1.410	E_{compr} calc.
Mm	$2.01588 * 10^{-3}$ kg/mole	E_{compr} calc.
R	8.3145 J $K^{-1}$$mole^{-1}$	E_{compr} calc.
LHV_{H_2}	33.33 kWh/kg	Storage calc.
$p_{saltCavern}$	180 bar	Storage calc.
$p_{pressureVessel}$	350 bar	Storage calc.
$p_{pipelineTransportation}$	100 bar	Storage calc.

Table 5.3: Constants for calculating the pressure drop in a pipeline.

Parameter	value	unit
D	30	inches
e	0.02*10^{-3}	m
μ_{H_2}	0.84*10^{-5}	Pa s

5.3 Offshore hydrogen production including storage

The area needed for a 1400 MW electrolyser has been estimated after a conversation with Sintef's Anders Ødegård. He is a part of the REFHYNE II, which will be the world's largest PEM electrolyser. It has a capacity of 100 MW and is located in Rheinland in Germany [43]. He could inform that the area of one cell with a capacity of 10 MW was ∼20x20 m^2. Another ∼20x20m^2 per 10 MW was needed to have space for the compatibility systems, like compressors. He informed that this area was not 100% scalable and could be smaller if necessary due to shareable technology between the 10 MW modules. In this case, the area needed for the 1400 MW electrolyser is estimated to be 56,000 m^2. The same area is needed for the compressor

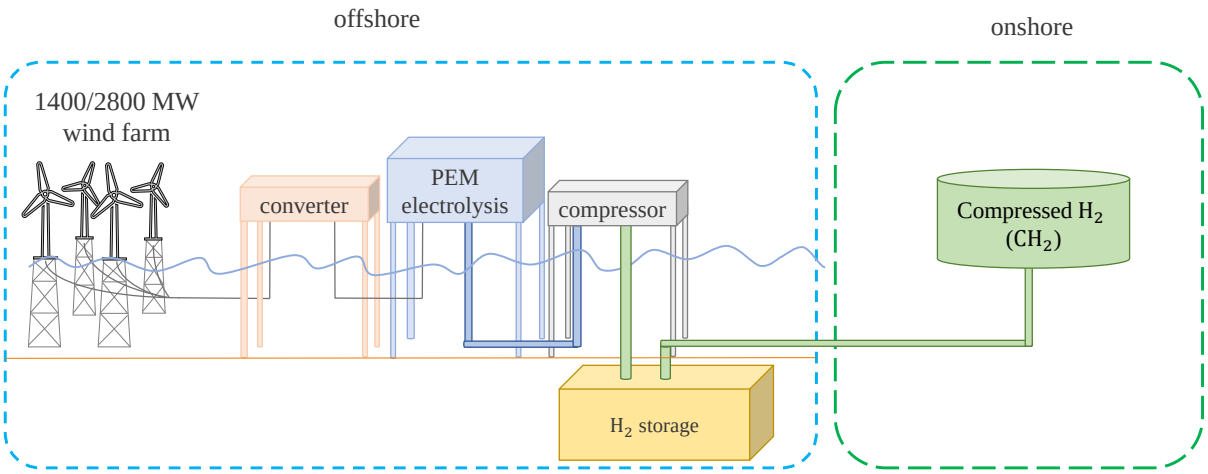

Figure 5.2: Visualisation of the base case with an added hydrogen storage.

with other compatibility systems.

When the electricity is generated at the offshore wind farm, it is converted and supplied directly to the electrolyser. The gas is compressed from 30 bar in production to the storage pressure or the transportation pressure and is transported through pipelines to shore 200 km away. The remaining, or lacking, is stored or withdrawn from the offshore storage. See figure 5.2 for a visualisation of the offshore wind to hydrogen model with integrated hydrogen storage.

The increase of pressure to equalise the losses in transport and the compression energy for storage are excluded in the total energy calculations for the cases with hydrogen storage. Other energy-demanding processes, like the demand for seawater desalination or adding or withdrawing hydrogen gas from the storage, are assumed to be negligible in this large scale power plant. However, the losses in the process before the electrolyser platform, being the losses in the cable from the wind power plant and the converter, is included in all of the calculations. In other words, if the wind power plant has a maximum capacity of 1400 MW, is the electrolyser supplied with 1358 MW. On the other hand, is the input power in the electrolysis referred to 1400 MW in the text of this thesis, but in the calculations, is it 1348 MW.

The storage solution in this model is not specified but is chosen to be either subsea storage tanks or subsea salt caverns. It is due to the fact that there are no operating subsea hydrogen storage in salt caverns or in subsea pressure tanks by 2022. Planned projects will gain important experience. Both the salt caverns and pressure tanks considered are located offshore and subsea to minimise the platform demand. The main difference between the two solutions is the storage pressure, the amount of base gas needed, and the cost. Section 4 present a further state of the art discussion and comparison of compressed hydrogen storage options in the Southern North Sea II.

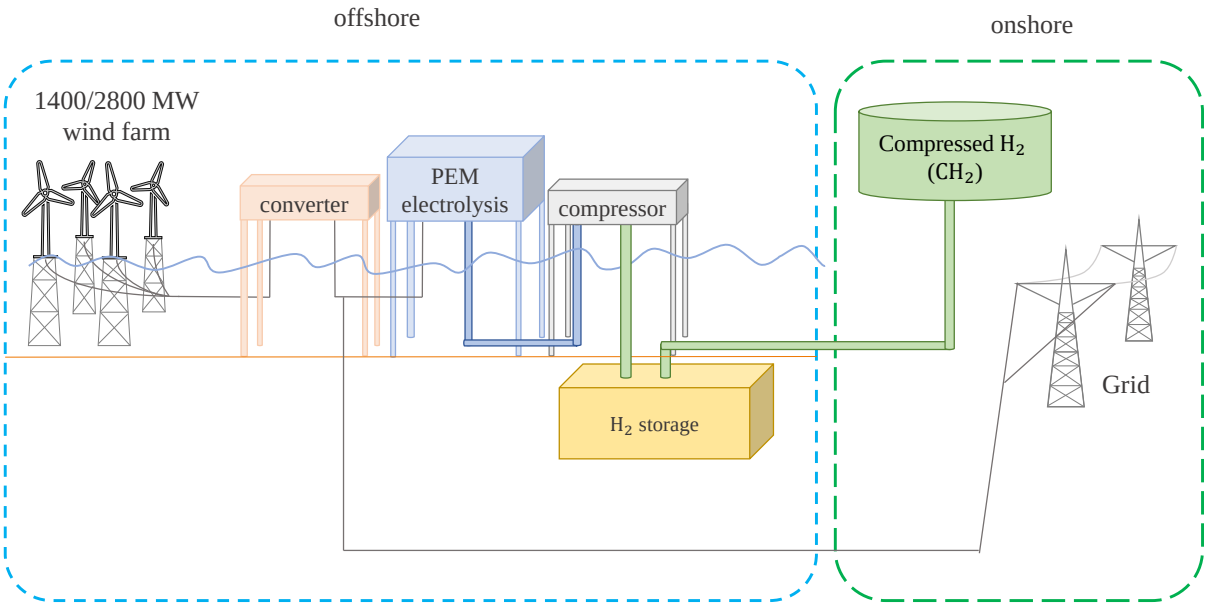

Figure 5.3: Visualisation of the base case with an added hydrogen storage and a grid connection.

The hydrogen demand at the shore is calculated as the mean produced in a particular time interval. The time intervals in this model are a constant yearly interval, monthly, 9.125 days, 5 days and 1 day interval for continuous delivery to shore.

5.3.1 Grid connection

The grid connection allows more flexibility in the model. The grid can both export and import power to export potential remaining power after hydrogen production and import power to the electrolyser in inconvenient weather conditions for wind power production. In other words, in this extension of the base model, it is not all of the power produced supplied to the electrolyser, but it has the flexibility to export and import power from the grid. The losses when power is transmitted through a cable to shore are excluded from the energy calculations.

The models which will be investigated are listed in table 5.4. The total wind power capacity and storage capacity vary. The aim is to investigate the power grid utilised for smaller storage capacities. In column four in table 5.4, the percentages of necessary storage are the fraction of the initial storage demand. The initial storage demand is the storage needed when delivering a continuous hydrogen delivery to shore in the belonging interval. There is no need for the grid when the storage has the initial storage size and the wind power capacity is 1400 MW. The storage size varies for the three interval divisions: yearly, monthly, and 9.125 days interval. When the grid is upscaled to 2800 MW, is the 100 % storage capacity the same as for the 1400 MW wind power plant with the corresponding interval division.

Table 5.4: The investigated combinations of component sizes. 100 % of the necessary storage is the storage needed if the combination of variables is not connected to the grid, and gives a constant delivery to shore in the given interval division.

Interval division	Wind power capacity [MW]	Grid capacity [MW]	percent of necessary storage
Year	1400	1400	100 %
Year	1400	1400	50 %
Year	1400	1400	10 %
Year	2800	1400	100 %
Year	2800	1400	50 %
Year	2800	1400	10 %
Month	1400	1400	100 %
Month	1400	1400	50 %
Month	1400	1400	10 %
Month	2800	1400	100 %
Month	2800	1400	50 %
Month	2800	1400	10 %
9.125 days	1400	1400	100 %
9.125 days	1400	1400	50 %
9.125 days	1400	1400	10 %
9.125 days	2800	1400	100 %
9.125 days	2800	1400	50 %
9.125 days	2800	1400	10 %

Table 6.1: The results from the project thesis written 2021, *Case study on hydrogen production from offshore wind power*, which underlie the following results of this master thesis.

Name	value
Wind power capacity	1400 MW
Wind power produced in 2019 at SNII	7382 GWh
Wind power capacity factor	60.25 %
H_2 produced offshore at platform	137,702,692 kg
Pressure loss H_2 pipeline	0.2 %
Compression energy amount (30 to 100 bars)	0.82 %

6 Results

The foundation of the model in this thesis is from the project thesis written in December 2021, named *Case study on hydrogen production from offshore wind power*. The modelled wind farm had a capacity of 1400 MW and was located at Southern North Sea II (SNII). The wind power plant produced 7382 GWh, corresponding to a capacity factor of 60.25 %. A study of Calado and Castro modelled a similar wind to hydrogen system with capacity of 1000 MW, and produced 432 tons/day which is 0.432 $ton/(day * MW)$, and the model in this thesis with a 1400 MW wind power capacity produced 614,16 tons/day which is 0.439 $tons/(day * MW)$ [34]. The weather data was from 2019, and the hydrogen produced was $137,702,692$ kg that year. The pressure loss was 0.2 % when the hydrogen gas was transported through pipelines to shore, which is ten times smaller than the energy loss when transporting current through HVDC cables, 2 %. Energy calculations showed that energy to compression of H_2 from 30 to 100 bar accounted for 0.82 % of produced energy in the wind power plant (WPP). See table 6.1 for an overview of the results from the project thesis, which underlie the results of this master thesis.

The establishment of 140 turbines is needed to reach the chosen capacity of 1400 MW in this model. The number of turbines require an area of 184.5 km^2, which is 7 % of the total area of the SNII. On a later stage, the model will double its capacity to become 2800 MW, and then 280 turbines are needed which require the total area of 369.0 km^2. It corresponds to 14 % of the total area of the SNII.

6.1 Offshore wind to hydrogen model with storage solution

6.1.1 Energy demand for compression to storage and desalination

If a salt deposit is the chosen solution for storage, which corresponds to a storage pressure of 180 bar, the energy demand for compression was 1.61 %. If a pressure vessel is the chosen technology, corresponding to a storage pressure at 350 bar, the energy amount for compression is 1.85 %. The pressure vessel could also store hydrogen in a small scale at 700 bar, and the compression energy needed would be 2.53 % of the total energy. The energy demand for compression is not included in the following results to have the flexibility of choosing storage solutions later.

The desalination process of salt water to freshwater of the total amount of produced hydrogen had an energy demand of 0.55 % of the total energy produced at the wind power plant. This energy is not included

Table 6.2: Hydrogen storage demand for distinct time intervals of constant delivery to shore. Interval for constant delivery to shore is the mean of the produced in the interval of observation, which is delivered to shore. The corresponding volume of the storage demand in a salt cavern and a pressure tank is also presented.

Interval for constant delivery in a year	max hydrogen stored	Volume pressure tank (350 bar)	Volume salt cavern (180 bar)
Year	8,071.43 tons	269,169 m^3	523,384 m^3
month	2,231.85 tons	74,428.6 m^3	144,722 m^3
9.12 days	1,587.64 tons	36,434.4 m^3	70,844.6 m^3
5.0 days	1,010.13 tons	17,461.8 m^3	33,953.6 m^3
1.0 day	227.404 tons	3,804.26 m^3	7,397.18 m^3

in the following calculations due to the minimal energy demand.

The wind to hydrogen power model has a storage solution integrated. The intervals for continuous delivery to shore vary to investigate the storage size demand. The following results correspond to the model visualised in figure 5.2 in section 5.3. The offshore wind and electrolyser have a capacity of 1400 MW with a storage solution of indefinite size and design. The hydrogen is sent to shore by pipelines. With the basis of previous work, the model had a mean hourly production of 15.7 tons per hour over the year 2019.

Table 6.2 shows the corresponding volumes for distinct storage technology solutions and the belonging interval divisions. The interval divisions are further presented in the following section.

6.1.2 Yearly constant interval

Figure 6.1 shows the hydrogen storage demand and the belonging duration curve for a constant delivery to shore through the whole year. The total storage capacity, in this case, is 8,071 tons. The volume of the salt cavern is the same as a cubic box with sides of 81 meters in length, while the demanded volume in a pressure vessel is the same as a cubic box of 65 meters. The curve is shifted in order to maintain a positive storage status. The amount of hydrogen that needs to be stored in the previous year is approximately 3000 tons. The storage refills during winter and withdraws throughout the summer. It refills again in late November. It has the same amount of hydrogen stored at the start and end of the year—this case with a constant yearly delivery to shore supply of 15.7 tons each hour to shore.

6.1.3 Monthly constant interval

The year was divided into months, with continuous delivery to shore each month, and figure 6.2 shows the resulting storage status. It also shows the belonging duration curve. The storage status in each of the months varies in shape, but similar for all of the intervals is that the amount of hydrogen at the start of the interval is the same as the amount at the end of the interval. The mean delivery to shore is written in the labels for each month, but the mean of these is still 15.7 tons. The delivery to shore also varies, with a higher delivery in the winter compared to the summer. The initial storage level needs to be 902 tons to have enough hydrogen to serve the calculated hydrogen demand. 902 tons account for 40 % of the total storage capacity.

Figure 6.1: Storage status a hydrogen storage connected to a modelled offshore wind and hydrogen power plant, both of 1400 MW capacity. This case have a constant delivery to shore every hour in the whole year. The delivery to shore was 15.7 tons each hour.

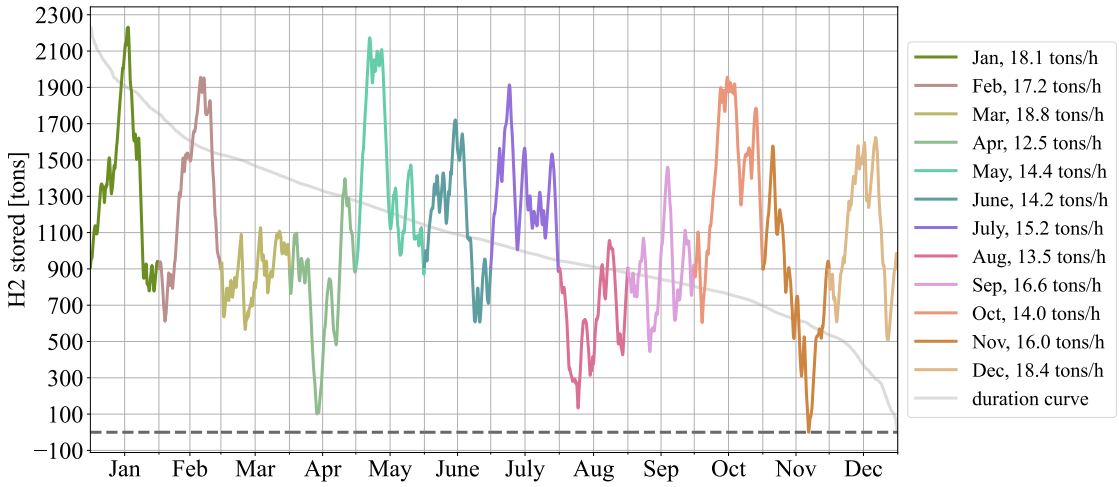

Figure 6.2: Storage status of the modelled hydrogen storage, which is connected to a modelled offshore wind and hydrogen power plant of capacity of 1400 MW each. This case has a constant delivery to shore every day in each month of the year. The delivery to shore therefore varies each month, but the supply amount each hour is written in the label in the right of the plot.

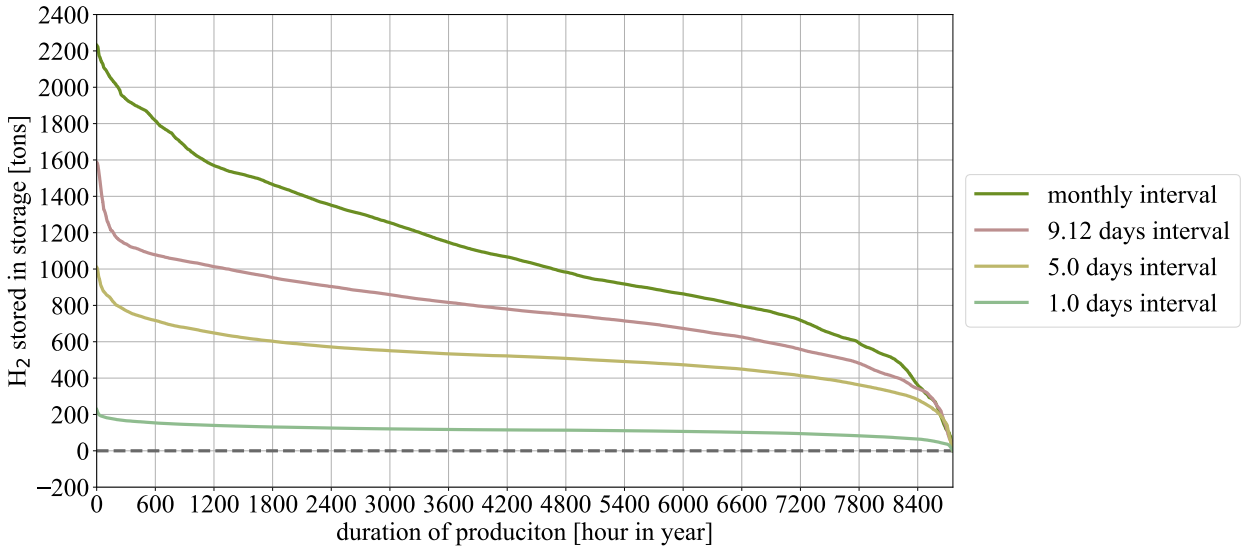

Figure 6.3: Duration curve of the storage status of the H_2-gas which needs to be stored in order to have a constant delivery to shore in the time intervals mentioned in the corresponding labels.

6.1.4 9.125 days, 5 days and 1 day intervals

Table 6.2 presents the hydrogen storage demand needed to deliver a constant flow of hydrogen in time intervals of 9.125 days, 5 days and 1 day interval. It also shows the storage demand for the already mentioned intervals of a year and a month. The same table shows the corresponding volume of the storage demand in a pressure tank or a salt cavern. The volume for the yearly interval with pressure tank solution is the same as for a cubic box of 60 meters side length. The volume for the 1 day interval for a salt cavern and a pressure tank corresponds to a cubic box of 19 meters side length and 15 meters side length, respectively. The belonging duration curves for the same intervals are shown in figure 6.3. The storage demand decrease for smaller intervals of continuous delivery to shore.

6.2 Grid integration and upscaled wind power plant

A grid is integrated to add more flexibility to the model. The wind power is upscaled to 2800 MW in some of the model cases to observe the utilisation of the already existing components.

Table 6.3 shows an overview of all of the combination of the component sizes which is investigated and its belonging figure of the plot of the electrolyser power, grid power and the storage status. It also shows the percentage of dumped energy compared to the total wind power production. The table presents the working storage, which is the storage volume where the total storage level has reached. A graphical visualisation of the working storage is the volume of the gas between the top and the bottom of the storage status curve. The table shows the number of hours where the electrolyser start and stops and the count of the hours where there has been no transmission in the grid meant for export and import. All of the model combinations are shown in table 6.3 supplied all of the hydrogen demand, which was set up as the mean of the produced hydrogen in the interval of consideration.

Table 6.3: Component sizes combination and additional results from the analysis of the wind to hydrogen model with grid connection. The figure number is the figure where the results from the electrolyser power, grid power and storage status is plotted. E_{dumped} is the amount of dumped energy in the distinct case and is presented as a fraction of the produced energy at the WPP. *Working storage* is the percentage of the difference of the top and bottom of the hydrogen storage level compared to the total storage capacity. Meaning the amount of storage where gas have either been added or withdrawn to reach. E.g. means 11 % working storage that the storage level have reached (100 % - 11 % =) 89 % of the total storage capacity at a minimum. *Count start/stop ELSY* is the amount of times the electrolyser stop and start again and the *Count hour free capacity in grid* is the number of hours where there is no transmission in the grid for import and export.

Interval div.	P_{wind} [MW]	P_{grid} [MW]	Storage capacity	Fig. number	E_{dump} [%]	Working storage [%]	Count start/ stop ELSY	Count hour free cap. in grid
Year	1400	1400	100 %	6.5	0.0	100.0	98	8,760
Year	1400	1400	50 %	6.5	0.0	100.0	92	7,849
Year	1400	1400	10 %	6.5	0.0	100.0	72	6,546
Year	2800	1400	100 %	6.6	5.26	11.38	55	2,333
Year	2800	1400	50 %	6.6	5.26	22.75	55	2,333
Year	2800	1400	10 %	6.6	5.29	100.0	54	2,319
Month	1400	1400	100 %	6.7	0.0	100.0	98	8,760
Month	1400	1400	50 %	6.7	0.0	100.0	95	7,839
Month	1400	1400	10 %	6.7	0.0	100.0	32	4,870
Month	2800	1400	100 %	6.8	4.75	35.97	55	2,255
Month	2800	1400	50 %	6.8	4.75	71.94	55	2,255
Month	2800	1400	10 %	6.8	5.05	100.0	40	1,773
9.125 days	1400	1400	100 %	6.9	0.0	100.0	98	8,760
9.125 days	1400	1400	50 %	6.9	0.0	100.0	86	8,311
9.125 days	1400	1400	10 %	6.9	0.0	100.0	22	4,654
9.125 days	2800	1400	100 %	6.10	4.26	43.69	55	2,170
9.125 days	2800	1400	50 %	6.10	4.26	87.38	55	2,170
9.125 days	2800	1400	10 %	6.10	4.66	100.0	29	1,634

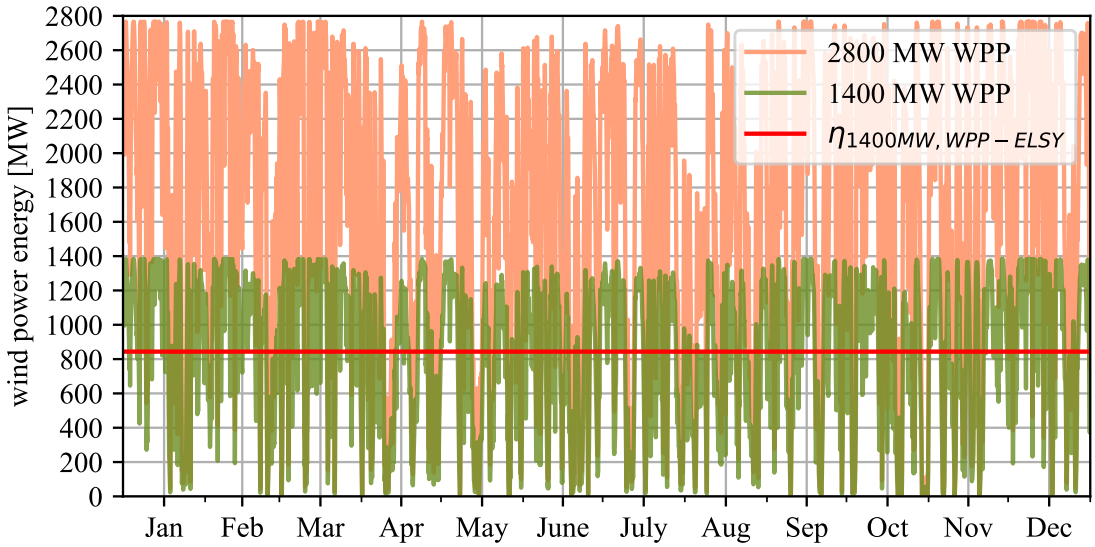

Figure 6.4: The wind power curve of a 1400 MW wind power plant and its mean capacity factor, $\eta_{1400MW,WPP-ELSY}$, which is the energy delivered to the electrolyser. In some combination cases, the wind power plant is increased to 2800 MW, while the electrolyser stays at 1400 MW. The wind power curve for the 2800 WPP is plotted as well. The wind speed needed to reach the capacity factor of the 1400 MW WPP is, therefore, smaller for the 2800 MW WPP than for the one of 1400 MW.

Figure 6.4 shows a comparison of the 1400 MW offshore wind power plant and its mean capacity factor, which is the same as the power supplied to the 1400 MW electrolyser. The wind power curve for the 2800 MW wind power plant is also plotted and compares the capacity factor of the 1400 MW wind power curve, the electrolyser, and the wind power curve for the 2800 MW.

6.2.1 Year interval

Figure 6.5 shows the result of the model with a constant delivery to shore through the whole year. The wind power plant has a capacity of 1400 MW, and it has a grid connection. The hydrogen storage capacities vary from 100 % to 50 % and 10 % capacity. The 100 % capacity corresponds to the storage capacity needed to supply a continuous hydrogen delivery each hour throughout the year. The electrolyser power, grid power and storage status are plotted for the three sizes of the storage capacity.

The case with a 100 % storage capacity is the same as the case in figure 6.1. It is due to the initial conditions being the same: the wind power capacity, hydrogen storage capacity, and electrolyser capacity. The grid is connected but is not necessary nor utilised in this case.

The electrolyser power is displaced where the power is 0.8 GW when the storage capacity decrease. The value of 0.8 GW corresponds to the threshold value where the electrolyser only produces hydrogen to supply the demand, being 60.25 % of the total capacity of the electrolyser. The displacement on the right and left side of the line represents the import and export of power to the electrolyser. The electrolyser starts and stop between 72 and 98 for the varying storage capacity cases.

Decreasing hydrogen storage capacity leads to an increasing grid import and export. There are still many hours when there is no transmission in the grid. The total export power were 132.8 GWh and 431 GWh, while the total import power was 209 and 453 GWh for the 50 % and 10 % storage capacity cases, respectively. Table 6.3 shows the number of hours of free capacity being 8760, 7849 and 6546 for the cases of 100 %, 50 % and 10 % storage capacity. There is no power dumping in either of the component size combinations shown in figure 6.1.

The storage status of the three cases is shown in the third plot of figure 6.1. All of the cases shown in the figure utilise all of the storage capacity and have a working storage of 100 %, see table 6.3. The graph for the 50 % and 10 % storage capacity has the same gradient as the storage status for 100 % storage capacity between the minimum and maximum storage capacity. When it is at the maximum storage capacity but still has remaining power, the remaining energy is exported. The decreasing storage capacity leads to an increase of export and import power since it reaches its maxima and minima more rapidly. It therefore have to export and import power to a higher degree. When the amount of stored hydrogen reaches the bottom of the storage, and if there are inconvenient weather conditions for power production, will the electrolyser produce hydrogen from imported power to meet the demand at the shore.

Figure 6.6 shows the result of the model with a constant delivery to shore but with a wind power capacity of 2800 MW. The grid and electrolyser have a 1400 MW capacity, and the storage varies from 100 % to 50 % and 10 % of the total storage demand for continuous delivery to shore. Therefore, the total storage capacity is the same in this plot and figure 6.6 with a 1400 MW wind power plant.

The electrolyser power is almost the same for the three cases even though they have changing total storage capacity. The case with 10 % storage capacity has an infinitesimal displacement at the threshold value. The electrolyser produces hydrogen at its threshold value when the hydrogen storage is full. The electrolyser power produces at its maximum of 1400 MW in 0 to approximately 1000 hour, and this energy amount is used to refill the storage to a maximum. From approximately 2000 hours to 7000 is the electrolyser at its threshold value, at 0.8 GW, and only produces the necessary hydrogen to fulfil the hydrogen demand. The potential remaining power after producing the hydrogen demand is exported to the grid. If the grid capacity is maximised, the rest of the energy will be dumped. The electrolyser has a count of start and stops of 54 for the case of 10 % storage capacity and 55 for the two other cases.

The second plot in figure 6.6 shows the grid import and export power. The grid import and export curve is the same for the case with 100 % and 50 % storage capacity. It is almost the same for the case with 10 % storage capacity but has some infinitesimal amount of import power. The case imports power from the grid when the hydrogen storage level is minima, and there is no available wind power to produce the hydrogen demand. The total amount of export power was 6414 GWh, 6414 GWh and 6415 GWh for the 100 %, 50 % and 10 % storage capacity cases, respectively. The total amount of import power was 0 for the 100 % and 50 % storage capacity case and 6.5 GWh for the 10 % storage capacity case. From 0 to around 2500 is the export capacity maximised. In this case produces the WPP enough energy to both fulfil the threshold value for production of the hydrogen demand, being 0.80 GW, and export the remaining power and maximise the grid capacity of 1.4 GW. Therefore, the wind power plant produces a minimum of 2.2 GW (1.4 GW + 0.8 GW), and if the wind power plant produces more, the rest of the energy is dumped. Table 6.3 shows the

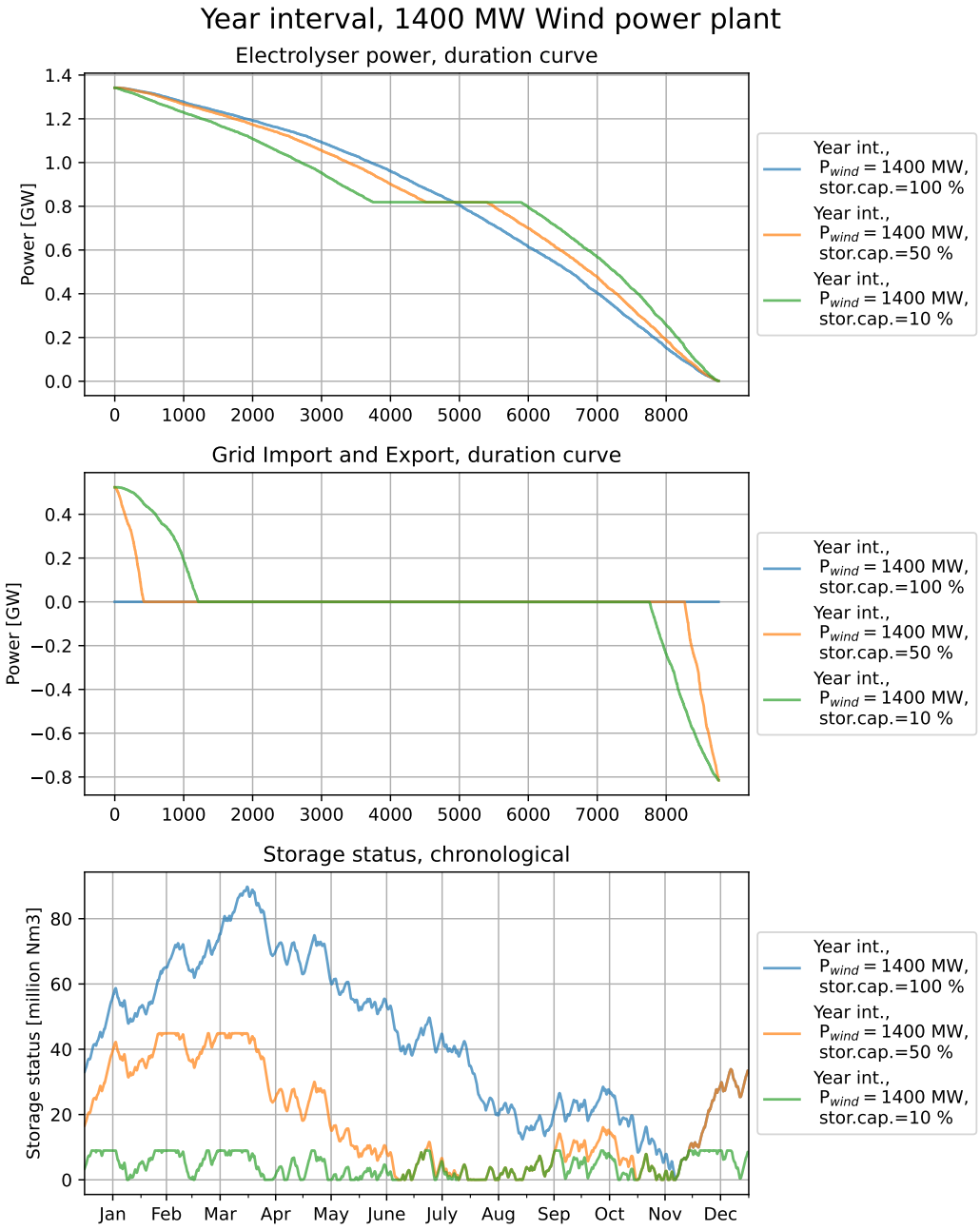

Figure 6.5: The plots show the electrolyser power, the grid import and export power and the hydrogen storage status of a model with both wind power capacity, electrolyser capacity and grid capacity of 1400 MW. The storage capacity varies from 100 % to 50 % and 10 % of the total storage demand for continuous delivery to shore through the whole year. The 100 % storage capacity corresponds to the storage demand to supply a constant hydrogen gas flow each hour throughout the year. The labels on the right side of the plots correspond to the interval, the wind power capacity and the percentage of the storage available in the particular case. Grid export is represented as a positive number, while imported power is represented as a negative number.

amount of dumped energy and is approximately 5.3 % for the three cases. The grid has no import nor export for 2,333 hours for the case of 100 % and 50 % storage capacity and 2,319 for the 10 % storage capacity case.

The storage status of the three cases of 100 %, 50 % and 10 % of the storage capacity with 2800 MW wind power are shown in the last plot in figure 6.6. The three plots for the three cases have the same gradient but shift according to the total amount of storage capacity. The storage amount is at its maximum in almost all of the year's hours in the case of 50 % and 100 % storage capacity. The two cases have working storage of 22.75 % and 11.38 %, respectively, which is the same amount of working storage volume. It means that the two cases have the same results, even though they have different total hydrogen storage capacities. The case with 10 % storage capacity has 100 % working storage.

6.2.2 Month interval

Figure 6.7 shows the electrolyser power, grid import and export and storage status of the case with monthly intervals of continuous delivery to shore. The case with 100 % storage capacity is, therefore, the same as the storage case plotted in figure 6.2. It has an electrolyser and wind power of 1400 MW and the same storage capacity, but the storage has enough capacity, so it is not utilised.

The electrolyser power is displaced around the threshold values for decreasing hydrogen storage capacity. The electrolyser only produces the demand when it produces hydrogen at its threshold value. The threshold value will vary each month since the constant demand varies in the same rate. The decreased storage capacity increases the displacement, and the displacement around the threshold value is caused by the import and export power. The count of start and stops in the electrolyser is 32, 95 and 95 of the 10 %, 50 % and 100 % storage capacity, respectively.

The grid import and export increase for decreasing storage capacity. The total amount of exported power was 169 GWh and 740 GWh and the total amount of imported power was 166 GWh and 743 GWh for the 50 % and 10 % storage capacity case, respectively. There are still hours of free capacity in the grid even though the hydrogen storage capacity decreases from 100 %. In the case of 50 % and 10 % storage capacity, is it 7,839 and 4,870 hours of free capacity, respectively. There is no power dumping in all of the storage capacity cases, shown in figure 6.7.

The storage status of the case with 100 % storage capacity is the same as the plot in figure 6.2. The case with a storage capacity of 50 % and 10 % has the same gradient as the case with 100 %, except when it reaches the maximum and minimum storage capacity. If the hydrogen in the storage reaches the maximum of the storage, the potential remaining power is exported through the grid. If the storage reaches the minimum, power is imported to supply the hydrogen demand. The case of 10 % storage capacity imports and export power to a higher degree since it has a smaller storage capacity and reaches the maxima and minima more often.

Figure 6.8 shows the case with continuous monthly delivery to shore, but a 2800 MW wind power plant supplies the electrolyser. The electrolyser and grid power curves overlap for the case with 100 % and 50 % storage capacity.

The plots for the electrolyser power and grid import and export of the case of 10 % storage capacity

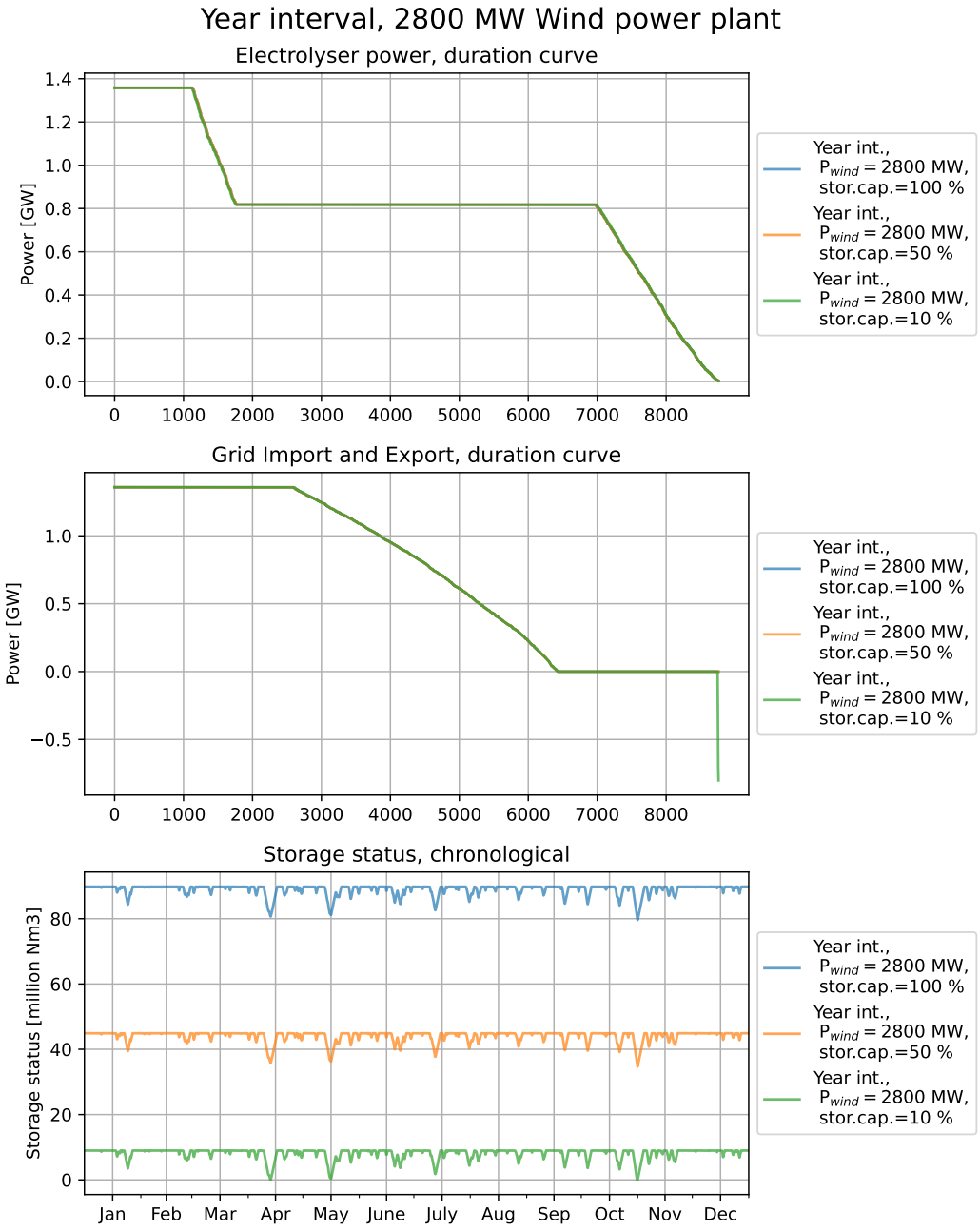

Figure 6.6: The plots show the electrolyser power, the grid import and export power and the hydrogen storage status of a model with wind power capacity of 2800 MW and electrolyser capacity and grid capacity of 1400 MW. The storage capacity varies from 100 % to 50 % and 10 % of the total storage demand for continuous delivery to shore through the whole year. The 100 % storage capacity corresponds to the storage demand to supply a constant hydrogen gas flow each hour throughout the whole year. The labels on the right side of the plots correspond to the interval, the wind power capacity and the percentage of the storage available in the particular case. Grid export is represented as a positive number, while imported power is represented as a negative number.

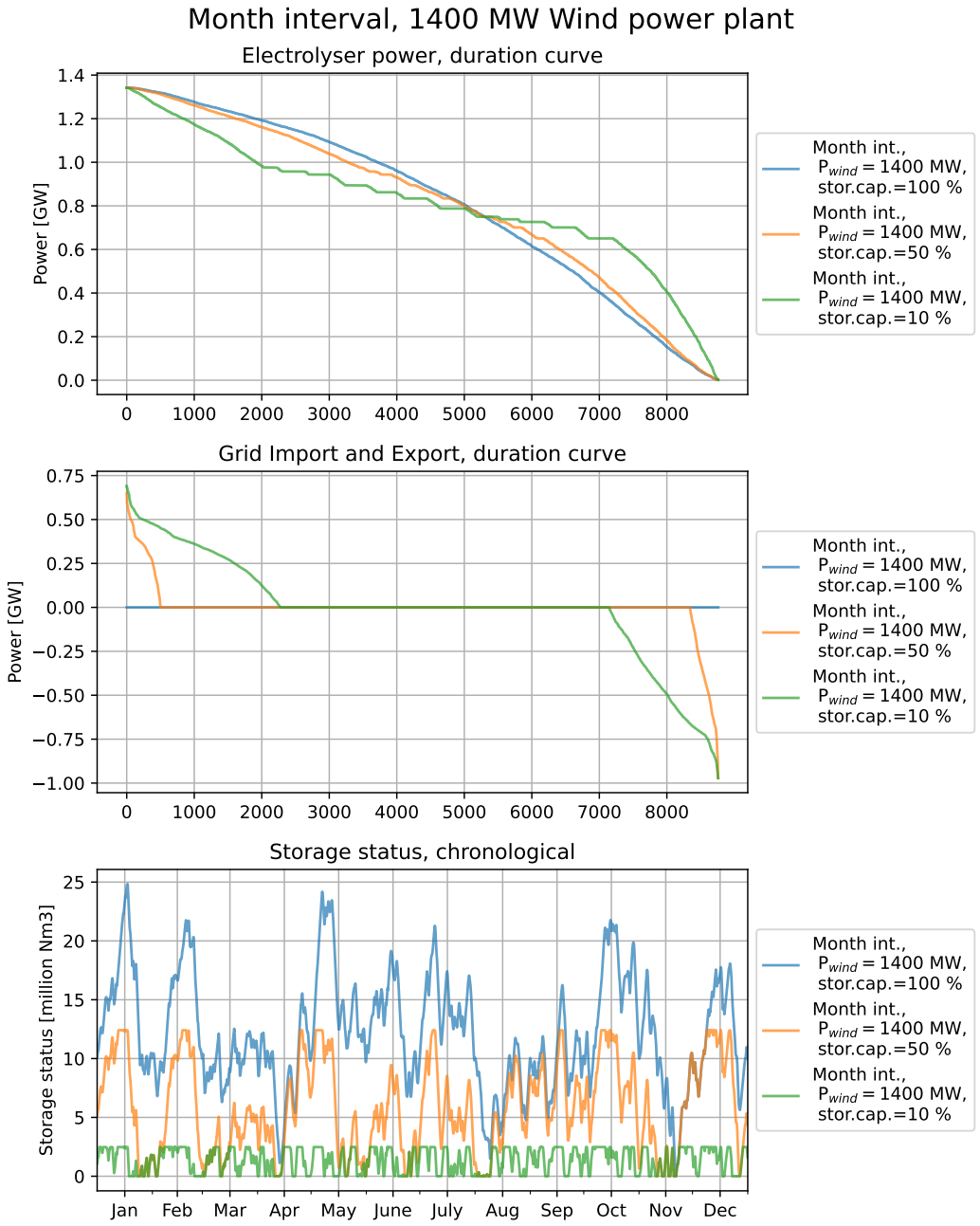

Figure 6.7: The plots show the electrolyser power, the grid import and export power and the hydrogen storage status of a model with wind power capacity, electrolyser capacity and grid capacity of 1400 MW. The storage capacity varies from 100 % to 50 % and 10 % of the total storage demand for a year with a constant monthly delivery to shore. The 100 % storage capacity corresponds to the storage demand to supply a constant hydrogen gas flow each month. The labels on the right side of the plots correspond to the interval, the wind power capacity and the percentage of the storage available in the particular case. Grid export is represented as a positive number, while imported power is represented as a negative number.

have a slight shift. The electrolyser produces at its maximum from hour 0 to approximately hour 1000, and refills the storage in this amount of time. Like the previous case of 1400 MW wind power but continuous monthly delivery, the electrolyser has a varying threshold value due to the constant demand each month. The electrolyser power curve increases the length of the threshold value production when the storage has a 10 % capacity. The electrolyser produces hydrogen at its threshold value when the hydrogen storage is full and has remaining power from the WPP. Hydrogen is not withdrawn from the storage to fulfil the demand but rather created in the electrolyser due to the priorities of the control strategy of the simulation tool. The remaining power is exported to the grid. The electrolyser start and stops 40 times for the case of 10 % storage capacity and 55 times for the two other cases.

The grid import and export power curves are identical for the cases with 100 % and 50 % hydrogen storage capacities. When the grid export is at its maxima, produce the wind power plant has enough energy to supply the hydrogen demand and export 1400 MW of power. In this case, the storage can be full, and wind power produces hydrogen at its threshold value that month and exports 1400 MW and dump the rest of the power if some remains. The wind power plant can also produce at its maxima of 2400 MW and transmit 1400 MW to the electrolyser to refill the storage and export the remaining 1400 MW through the grid. 6487 GWh was totally exported in the 100 % and 50 % storage capacity case, while 6645 GWh and 200 GWh was totally exported and imported in the 10 % case. 5.05 % of the energy was dumped in the 10 % storage capacity case and 4.75 % in the two other cases. There is some free capacity in the grid being 1,773 hours in the 10 % storage capacity case and 2,255 hours in the two other cases.

The storage status curves for the three storage capacity cases are shown in the third plot in figure 6.8. The 50 % and 100 % storage capacity case has the same curve. It has only been shifted due to the total capacity. The case of 50 % and 100 % storage capacity has working storage of 35.99 % and 71.94 %, respectively, which is the same storage volume. The case of 10 % storage capacity has the same gradient as the two others between the maximum and minimum of the storage. It imports power when there is no more hydrogen left in the storage and not enough wind power to supply the threshold value for hydrogen demanded production that month.

6.2.3 9.125 days interval

Figure 6.9 shows the result of the analysis with a constant delivery to the shore of 9.125 days and power curve of a 1400 MW wind power plant, grid and electrolyser. Electrolyser power curve for the case of 100 % and 50 % storage capacity almost overlap. However, there is a slight shift around the threshold values for the intervals, which is more clearly visible in the case of the 10 % storage capacity. The decrease of the interval duration for continuous delivery leads to more intervals in a year, making the curve by threshold values shift more smooth than the monthly and yearly case. The electrolyser starts and stops 98, 86 and 22 times for the cases of 100 %, 50 % and 10 % storage capacity, respectively.

The grid import and export increase for a decrease of storage capacity. At the same time, the import and export power of the 50 % storage capacity case is minimal, and there are 8,311 hours of free capacity in the grid. It increases for the 10 % storage capacity case, but there are still 4,654 hours of free capacity in the grid. The total amount of exported power was 69 GWh and 752 GWh in the 50 % and 10 % storage capacity

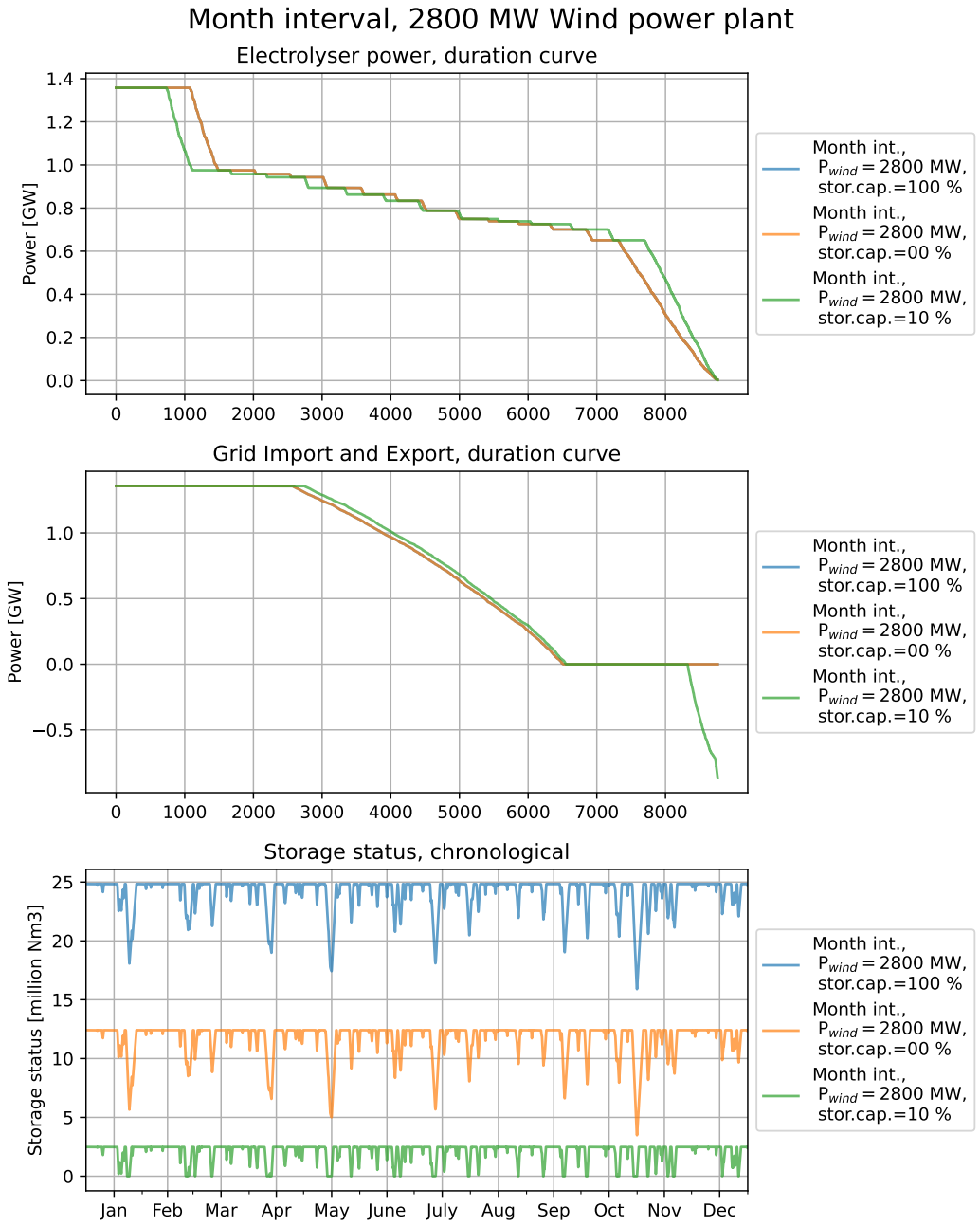

Figure 6.8: The plots show the electrolyser power, the grid import and export power and the hydrogen storage status of a model with wind power capacity of 2800 MW and electrolyser capacity and grid capacity of 1400 MW. The storage capacity varies from 100 % to 50 % and 10 % of the total storage demand for a year with continuous monthly delivery to shore. The 100 % storage capacity corresponds to the storage demand to supply a constant hydrogen gas flow each month. The labels on the right side of the plots correspond to the interval, the wind power capacity and the percentage of the storage available in the particular case. Grid export is represented as a positive number, while imported power is represented as a negative number.

case. There were 86 GWh and 755 GWh imported power in the 50 % and 10 % storage capacity case. There is no power dumping in these cases with 1400 MW wind power plant and 9.125 days interval for continuous delivery.

The storage status curves for the 100 % and 50 % storage capacities are similar but shifted according to the maximum storage capacities. The curve for 100 % storage capacity fluctuates around approximately 8.5 million Nm3 and has one defining top in September, determining the 100 % storage size. The storage minimum is between October, November, and December defines the storage minimum. The case of 50 % is very similar but has cropped tops and bottoms when the storage capacity is maximised or minimised, respectively. The case of 10 % storage capacity fluctuates the storage level rapidly between the top and bottom of the storage. In this case, it imports power when the storage is empty, and it needs to produce the hydrogen demand. It exports power when the hydrogen storage is full, and there is not enough power from the WPP to supply the threshold value of the month. The working storage of all of the cases is 100 %.

Figure 6.10 shows the electrolyser power, grid power and storage status of the case of continuous delivery to shore in 9.125 days and the effect of decreasing the storage to 50 % and 10 % of the initial storage capacity. The electrolyser power and grid import and export plots overlap for 100 % and 50 % storage capacity. The electrolyser power is maximised from 0 to 1000 hours, and refill the storage in these hours. After that, it stays at the threshold values until around 8000 hours, producing only the hydrogen demand at these hours and exporting the remaining energy. The 10 % storage capacity case slightly shifts to the left and the right due to the increased import and export power and produces hydrogen at its threshold value for longer time intervals. The electrolyser start and stops 29 times for the case of 10 % storage capacity and 55 times for the two others.

The grid export is maximised from hour 0 to approximately 2500 hours. In this case, the wind power is either higher than the sum of the grid export capacity and the threshold value for the interval of consideration. If it is more, will the rest be dumped. The amount of dumped energy is 4.26 % in all three storage capacity cases. The total amount of exported power was 6557 GWh in the 100 % and 50 % case, and 222 GWh was imported in the 10 % storage capacity case. There is also a small amount of free capacity in the grid, being 1,634 for the 10 % storage capacity case and 2,170 hours for the two others.

The storage status curves have the same shape but are shifted according to the maximal storage capacity. The working storage is 43.69 % and 87.38 % for the 100 % and 50 % storage capacity, corresponding to the same working storage volume. The storage status curve fluctuates to a higher degree between the top and bottom in the case of 10 % storage capacity and import and export power more than in the two other cases. It has working storage of 100 %.

6.3 Salt cavern storage potential in the Norwegian North Sea

According to Caglayan et al. is the salt cavern potential 7500 TWh in the Norwegian North Sea territory for storage of hydrogen in underground salt caverns [24]. A visualisation of the geological distribution is found in figure 4.2. The results from using the method described in chapter 3.3.2 is shown in table 6.4. The pot P_{wind} is the potential capacity of a wind power plant which supplies an electrolyser of the same size and has a storage capacity of the same size of the $m_{workinggas}$. The calculations gave a P_{wind} of 39.57

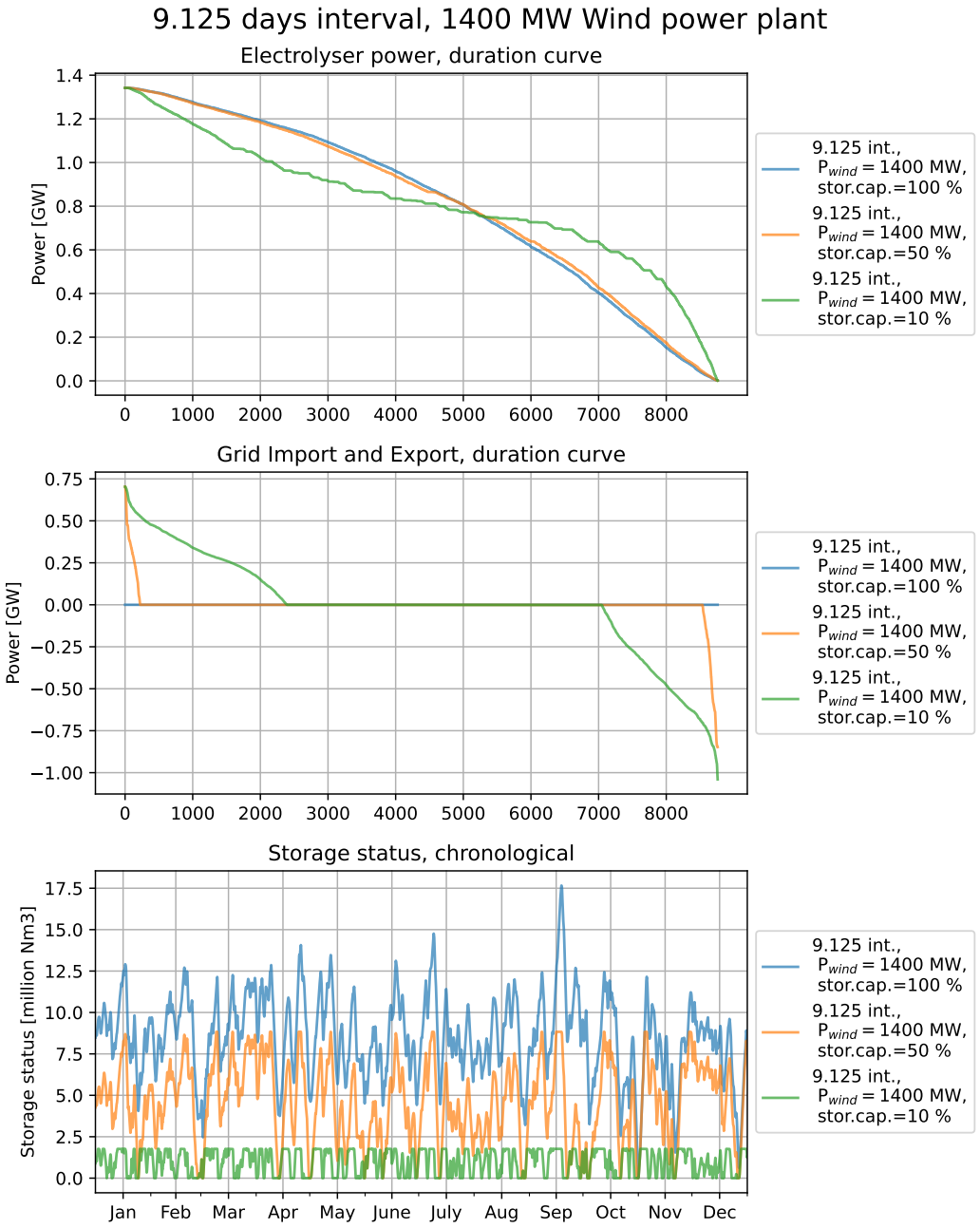

Figure 6.9: The plots show the electrolyser power, the grid import and export power and the hydrogen storage status of a model with wind power capacity, electrolyser capacity and grid capacity of 1400 MW. The storage capacity varies from 100 % to 50 % and 10 % of the total storage demand for a year with 9.125 days of continuous delivery to shore. The 100 % storage capacity corresponds to the storage demand to supply a constant hydrogen gas flow every 9.125 days. The labels on the right side of the plots correspond to the interval, the wind power capacity and the percentage of the storage available in the particular case. Grid export is represented as a positive number, while imported power is represented as a negative number.

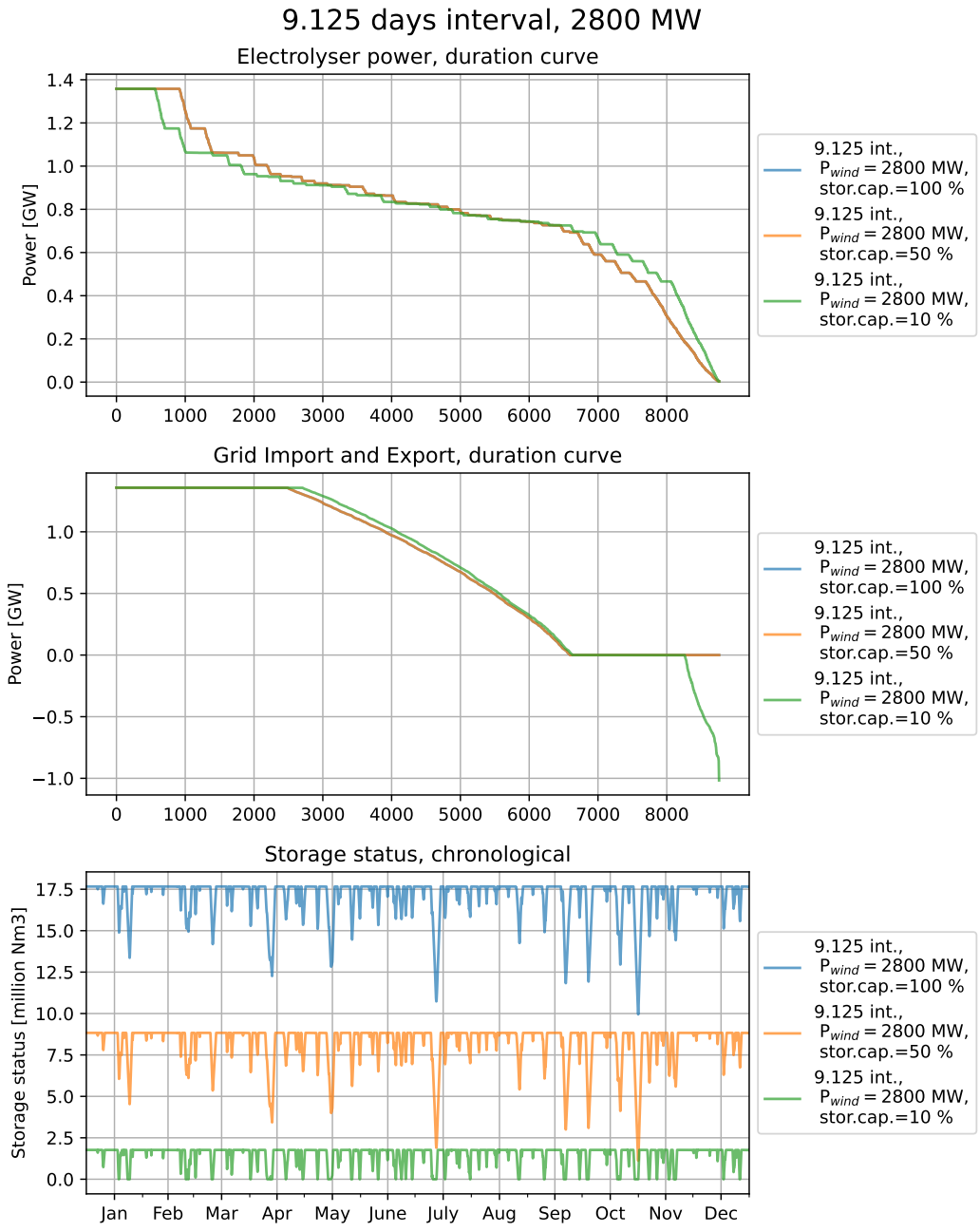

Figure 6.10: The plots show the electrolyser power, the grid import and export power and the hydrogen storage status of a model with wind power capacity of 2800 MW and electrolyser capacity and grid capacity of 1400 MW. The storage capacity varies from 100 % to 50 % and 10 % of the total storage demand for a year with 9.125 days interval of constant delivery to shore. The 100 % storage capacity corresponds to the storage demand to supply a constant hydrogen gas flow in 9.125 days each. The labels on the right side of the plots correspond to the interval, the wind power capacity and the percentage of the storage available in the particular case. Grid export is represented as a positive number, while imported power is represented as a negative number.

Table 6.4: Hydrogen storage potential in salt caverns according to the potential written in article by Caglayan et al. [24]. Location of all of the salt caverns is subsea.

cavern pot.[24]	$m_{workgas}$ [tons]	pot. P_{wind}	Total hydrogen energy produced	H_2 delivered to shore each hour	Area WT_{10MW}	Area ELSY plat.
7500 TWh	225*10^6	39.57 TW	128,080 TWh	439,071 tons	20.9*10^6 km^2	1582.8 km^2

TW and a $m_{workinggas}$ of 225*10^6 tons. The wind to hydrogen system produces hydrogen throughout the year, corresponding to 128,080 TWh of hydrogen energy. Compared, the world energy consumption is the produced hydrogen energy five times the world energy consumption. The area of the wind power plant is 20,860,088 km^2 accounting for 1.02 % of the area of the earth. This same area is 10 times the area of the sea territory of Norway, which is 1,979,179 km^2. This wind to hydrogen system delivers hydrogen to the shore each hour, corresponding to 432,071 tons. The same is for the electrolyser platform, which would be four times the size of the area of Trondheim city. When all of the potential storage capacity is utilised, the amount of hydrogen produced is 385 times the hydrogen aim in Europe in 2030.

7 Discussion

7.1 Offshore wind to hydrogen at SNII

The weather data imported from `renewables.ninja` was used to model and calculate the wind power production. The data was available from 2019. Including data from several years could make the power production calculations more reliable. Another factor which could improve the reliability of the results would be to consider the possible weather changes in the area of consideration of the potential wind power plant. The program collects data from the point of coordinate and not an area. Including weather data from other years and several spots from the potential area would give a more reliable result.

The approach from the PhD of Magnus Korpås was the basis for calculating the amount of hydrogen produced [31]. It was based on linear conversion between the wind and hydrogen system components. The compressor and the cable losses could vary depending on temperature or other external factors. Including the variations in the losses could lead to a more precise analysis method and further a more detailed result.

The result and model from the project thesis, *Case study on hydrogen production from offshore wind power* is the basis for the model in this master thesis. The method and results from the project thesis are considered reasonable when comparing them to other similar studies. The study of Calado and Castro is compared in the the results in this thesis in section 6, and the produced amount of hydrogen tons each day per MW is similar to the case from [34]. Due to the similarities between the results, the project thesis model is considered reasonable to use as a base case for further investigation and development.

The calculated average annual capacity factor of the WPP is 60.25 %, which is a very high capacity factor for a wind power plant compared to, e.g. Hywind Scotland, a floating wind farm with a capacity of 53.8 % [12]. Hywind Scotland has floating wind turbines and is therefore located where the ocean is deeper than 60 meters. The weather is often considered rougher when the ocean is deeper, leading to a higher capacity factor than bottom-mounted wind power plants. At the same time, both technical improvements and geological weather variations could improve the capacity factor of the model in this thesis, making it more optimal than the capacity factor at Hywind Scotland.

The amount of area used for the wind turbines in this model is only 7 % and 14 % of the total area at SNII for the 1400 and 2800 MW wind power plant respectively. There is, therefore, enough area at the SNII to establish a further upscaling of the offshore wind power production in the area of consideration.

PEM electrolysers have never been installed and operational with 1400 MW capacity before. The largest scheduled operational plant in 2024 is the 100 MW Refhyne II project, located onshore. At the same time, the electrolyser technology is module-based, and upscaling is possible to some degree. Some changes may be applied to the system to make it operational when it is upscaled and located offshore, and the consequences of this may affect its efficiency.

7.1.1 Including hydrogen storage

The wind to hydrogen system model has not specified the hydrogen storage technology to have the flexibility of choosing solutions afterwords. The technologies considered the most promising subsea hydrogen storage

solutions in the North Sea are pressure vessels and salt caverns. The consequence of not choosing the storage technology is the potential change in the result due to the difference in the compression energy demand for storage, the amount of base gas volume, access to salt caverns, and economic differences. The compression energy demand for pressure vessels is higher than for salt caverns. Suppose the energy calculations include the compression energy demand for storage. Then, when the pressure vessel is the preferred storage solution, the amount of hydrogen will be less due to the increasing amount of energy for compression.

The energy calculation excludes the energy demand for compression for storage and transport, energy for adding and withdrawing gas from potential storage, energy for desalination, and other energy-demanding processes due to the assumed small changes in the result. Significantly, the compression energy demand is a small fraction of the total energy in the model. The energy required to compress the gas to 100 bar to transport the hydrogen gas through a pipeline was 0.82 %. The amount of energy for storage in the salt cavern was 1.61 %, and 1.85 % for storage in the pressure vessel. Therefore, the small fractions make it reasonable to not include energy demand in the energy calculations due to the small fractions.

The compression energy needed to adjust for the pressure losses in the pipeline is 0.2 % and is not included in the energy calculations either. Energy demand for adding and withdrawing hydrogen from the potential storage tank is a more uncertain. Hydrogen storage in subsea salt caverns or subsea pressure vessels has never been established or operated. The energy demand is not predictable with a high range of security, but using data from onshore hydrogen storage could give a guiding result. The energy demand for desalination is 0.55 % is considered infinitesimal in a model of this size.

The base gas is required to make it operational and depends on the storage solution. The salt cavern storage requires 33 % base gas, leading to an increased storage size of 33 %. The remaining results from the analysis will give the same result since the base gas is not withdrawn nor added to the storage during a year, and the storage status curve will only shift with the exact size of the base gas.

The pressure vessel's cost is six hundred times higher per kilowatt-hour of hydrogen compared to the salt cavern hydrogen storage. The storage pressure of salt caverns is 180 bar, while the storage pressure of pressure vessels from 2022 is 350 bar, being 1.94 times higher. A significantly decreased cost of the pressure vessel is needed to compete economically with the salt cavern storage solution. On the other hand, a salt cavern needs to exist where the hydrogen is created and stored, making the pressure vessel a more mobile solution. This thesis, considering the Southern North sea, has a great potential for storage in existing underground salt caverns, discussed in section 7.2.

The shorter interval for continuous delivery to shore demanded smaller storage volumes. The storage size decreased by 70 % when the delivery went from a yearly constant to a monthly constant interval. The storage further decreased by 30 % when the interval of continuous delivery went from monthly to 9.125 days. The storage level decreased by 33 % and 20 % when the interval went from 9.125 to 5 days and 5 days to 1 day, respectively. In other words, an increase in storage demand is a consequence of a predictable, constant delivery to the end-user. However, when the delivery to shore is constant over smaller intervals, the aim of making the variable renewable energy more reliable is less satisfied.

7.1.2 Grid integration and wind power upscale

The red line marks the capacity factor of the 1400 MW electrolyser in figure 6.4. The figure shows the wind power capacity of the 1400 MW and 2800 MW WPP. The necessary wind speed to supply the 1400 MW electrolyser is, therefore, less for the 2800 MW WPP compared to the 1400 MW WPP. Therefore, the upscaled wind power plant produces more than enough to cover the electrolysis power to supply the hydrogen demand. After supplying the electrolyser load, the remaining power of the upscaled wind power plant with 2800 MW capacity can be utilised for other purposes. In this model was the power exported to the power grid at shore.

The losses in the transmission of power to the shore are estimated to be 2 %. The loss is not included in the energy calculation of the cases with a grid connection to shore. It is due to the infinitesimal loss compared to the total energy production in the wind power plant.

7.1.2.1 1400 MW wind power plant

Many of the same tendencies for the model cases of the 1400 MW power capacity repeat for the yearly, monthly and 9.125 days interval division of a year. This section, therefore, compares the intervals against each other.

All model cases with a 1400 MW wind power plant have no power dumping. The combinations of component sizes with a wind power capacity of 1400 MW cannot dump power since the wind power capacity never exceeds the total capacity of the electrolyser and power grid. The electrolyser and power grid have a capacity of 1400 MW, respectively, and, therefore, 2800 MW in total. The results also show no energy dumping since all of the energy is firstly used to produce hydrogen and secondly exported if there is remaining power. On the other hand, power is imported if there are inconvenient wind power production conditions to fulfil the hydrogen demand. The imported power can be considered a loss in the energy calculation since the power is not from the power source in this model, which is the wind power production.

The 1400 MW wind power plant, with continuous delivery to shore throughout the whole year, increased grid import and export when the storage size decreased. The grid exported and imported in 10 % more hours when the hydrogen storage size decreased by 50 %. It exported and imported in 25 % more hours when the storage decreased to 10 %. There are still many hours when the grid is not transmitting power. Therefore, it is essential to compare the investment cost of the grid against its utilisation. The free grid capacity could be utilised for other purposes, like electrifying an oil and gas platform or transmitting power from another offshore power production spot. This potential grid utilisation can not collide with the original power transmitting to and from the electrolysis platform but shows a possible way to utilise the already installed grid in the model.

The monthly and 9.125 days continuous delivery with 1400 MW offshore wind power plant has the same tendency as the 1400 MW with yearly constant delivery interval, with increased grid import and export when the storage capacity decreases. A difference between the monthly and the 9.125 days interval compared to the continuous delivery in a year is that the grid import and export amount increase more when the hydrogen storage capacity decreases to 10 %. The amount of hours with grid import and export are increased by 50 %,

approximately double the import and export in the interval with continuous delivery through the year. It may be an effect caused by the increased variation in the amount of hydrogen in the storage due to the smaller intervals for continuous hydrogen delivery. In addition, the volume of the 100 % storage capacity case is smaller for the monthly and 9.125 days intervals. Therefore, the more rapidly varying hydrogen amount in the storage will meet the maximum and minimum more frequently, leading to more demand for import and export power when the storage capacity decreases to 50 % and 10 %.

7.1.2.2 2800 MW wind power plant

Many of the same tendencies for the model cases of the 2800 MW power plants repeat for the yearly, monthly and 9.125 days interval. This section compares the intervals against each other.

The upscaling of the wind power plant has minimal dumping of energy. It utilises almost all of the energy produced in the wind power plant for grid export and hydrogen production. The electrolyser has a capacity of 1400 MW, and the grid has a capacity of 1400 MW, making it 2800 MW in total. However, if the wind power plant produces near its maxima and has no storage capacity, the electrolyser produces hydrogen at its threshold value, supplying the demand. If there is enough power to export the maximum of 1400 MW, is the rest of the produced energy dumped. The amount of dumped energy is ~5 % of the total wind power in all cases where the wind power is 2800 MW. The amount of power dumping can be considered small. There is also only power import to hydrogen production in the cases of 10 % storage capacity in all of the intervals. These amounts, and the power dumping amounts, are minor, making the wind power up-scaling overall efficient.

The wind power capacity increase from 1400 MW to 2800 MW led to a smaller amount of *Working storage* for all of the interval cases with 100 % and 50 % initial storage capacity. The amount of storage volume demand, meaning the volume of the working storage, was the same for the cases with 100 % and 50 % storage capacity. It led to the same results for the electrolyser power curves and the grid power import in the cases with the same interval divisions. The storage status curves had the same shape but shifted according to the total storage capacity. The decrease in storage capacity demand is especially favourable if the hydrogen is stored in pressure vessels, being an expensive storage solution.

The case with 10 % storage capacity mainly exports power. There is also a small amount of imported power in these cases. The yearly interval had 11 % working gas in the 100 % storage capacity case. Therefore, the storage size is 1 % too small when the total storage capacity is later set to 10 %. Therefore, the case with 10 % needs to import power to supply the hydrogen demand. The same tendency is in the cases of monthly and 9.125 days intervals, but the working gas for the 100 % storage capacity case is 36 % and 43 %. It leads to a higher power import demand in the 10 % storage capacity case. There are only 1000 to 2300 hours of free capacity due to the main high export and import for the 10 % storage capacity case. It is, therefore, less favourable to utilise the grid for other purposes in these cases, compared to the 1400 MW WPP case.

The electrolyser has a decreasing amount of start and stops when the storage capacity decreases. It also decreases starts and stops when 2800 MW is the wind power capacity. The PEM electrolyser has an operating range of 0 - 100 %, and the amount of starts and stops is therefore not an issue in the first place. The PEM also reacts to changes in the input power after milliseconds, while AEL reacts after seconds. At

the same time, PEM is the most immature electrolyser technology for large-scale hydrogen production by 2022. If an AEL electrolyser is favourable to install in offshore wind to hydrogen system for other reasons, the operating range of 15-100 % would need to be taken into account. Therefore, choosing a model with the fewest start and stops would potentially be more favourable for getting an optimal solution.

7.1.2.3 Economic aspect of 2800 MW wind power

When upscaling the wind power capacity to 2800 MW are all other components kept the same size and model. The upscaling of the wind power plant lead to better utilisation of the components in the model, since more power is exported in addition to supplying the demand. It also results in a smaller demand for hydrogen storage and less power imported. The investment cost of the electrolyser, grid capacity, and other components are kept the same, except for the doubled cost of the wind power plant. From an economical analysis from the project thesis *Case study on hydrogen production from offshore wind power*, are the platform cost and the electrolyser cost the highest and most sensitive costs in the offshore hydrogen production case with 1400 MW WPP capacity. In other words, the upscaling of the wind power plant leads to higher utilisation of the already invested components and would, according to the results in the project thesis, not result in an extreme increase in the total investment cost. The higher utilisation is first and foremost the increased grid export.

7.2 Salt deposit potential in the North Sea

Hydrogen storage in subsea salt caverns in the Norwegian North Sea has colossal potential. Suppose the storage potential in the Norwegian North Sea territory is utilised. The modelled wind power plant, which would utilise all of the storage potentials, and supply an end-user at the shore with continuous delivery through the year, would have 39.57 TW of total capacity. The modelled electrolyser has the same capacity, and the total amount of hydrogen energy produced is 128,080 TWh of hydrogen energy. This energy amount is five times the world's energy consumption. In this case, the weather variations in the area of consideration for the wind power plant are essential since the total area of the result is 20,860,088 km^2, which is the same as 10 times the Norwegian Sea Territory.

It is also worth mentioning that establishing and building the wind power plant of size of the potential 39.57 TW capacity would be practically challenging due to the large areas for wind power plants and the areas. On the other hand, the results show the enormous potential of storing hydrogen gas in the salt caverns.

7.3 Further work

The calculation of the energy conversion between the wind power plant and the electrolysis has losses that are assumed to be linear. Further work could carry out the calculations of these losses in detail and the potential effects that could vary depending on external factors. The calculation of the start and stop of the electrolyser is investigated in the thesis and is one of many technical details to investigate further that could influence the result.

The control strategy of the model with grid integration in this thesis has hydrogen production and supplying the hydrogen demand as its priority. Suppose the hydrogen market evolves so that it is not a priority to supply hydrogen constantly, but the power from the wind power plant is more requested. The future hydrogen market is not possible to predict in detail, but if another control strategy matches the market better, it would be favourable to change the control strategy in the analysis. However, it remains for further work to evaluate how the market evolves and then adjust the control strategy to match the market.

The possibility of connecting the wind to hydrogen power plant to a potential offshore net can be studied further. The cases where the electrolyser and wind power plants have the same capacity have many hours with no transmission in the grid. The free capacity in the grid could be utilised for other purposes. When the wind power plant is upscaled, are a considerable amount of power exported to the grid. The grid connection in this model could also be a part of an offshore grid, even if the grid in this thesis was thought to be the main grid at the shore.

Comparing the technical results of the model components' dimensions and utilisation with the economic aspect remains for further work. Including the price for the grid connection establishment, prices of the storage solutions, and the potential power import and export price could be compared to the results. Then, the most optimal solution, both technical and economical, could be found. There is still a challenge with cost estimations. By 2022, a wind to hydrogen power plant of this size has never been established and operated. It, therefore, leads to insecure results. At the same time, much of the already existing technology is compatible offshore, which can lead to a hopefully guiding answer of which component sizes to choose for the most optimal combination of the economical and technical solution.

According to the results of this thesis, the subsea salt cavern hydrogen storage has great potential in the Norwegian territory. It remains to conduct technical analysis of the seabed. Compressed hydrogen has never been stored in salt caverns subsea, but Tractebel has an ongoing project which will do this. The experiences from the project will be valuable and essential for the utilisation of the storage potential in the Norwegian territory.

The wind to hydrogen system analysis should be considered again after further technical investigations of the seabed. If there is a enormous storage potential in the salt caverns would it lead to not needing to minimise the storage capacity. In that case, the grid could be excluded from the model, and a potential wind to the hydrogen power plant of the type modelled in this thesis could supply a constant hydrogen demand throughout the year. At the same time, this thesis discovered many advantages of upscaling the power plant. Suppose the possible excess power exported to the grid is more valuable than the investment cost of the grid capacity. Then, a grid connection and an upscaled power plant would be favourable. Regardless, a huge possible salt cavern storage potential would reduce the investment cost of the storage solution.

8 Conclusion

This thesis aimed to investigate the potential of combining offshore wind power production and offshore hydrogen production to make variable renewable energy more reliable. There is a significant potential for establishing wind power in the North Sea, and the modelled wind power plant in this thesis had a capacity factor of 60.25 %, which is a high utilisation factor. The combination of offshore wind and hydrogen production has not been established and operated before. However, the model in this thesis showed the potential and possibility of establishing the combine the two. This thesis also studies how an offshore storage solution could improve the predictability of the hydrogen delivery to shore. Shortening the interval for continuous delivery to shore led to a decreased necessary hydrogen storage demand. The two leading storage solutions of consideration in this thesis was the geological underground salt caverns and a subsea pressure tanks. The salt cavern technology offers low-cost storage, while the pressure tank has a higher storage pressure and higher hydrogen density. It remains to establish and operate subsea hydrogen storage. Planned projects with integrated subsea hydrogen storage exist but are not yet operational.

The grid was connected to the wind to hydrogen model to investigate the grid import and export transmission amount of a decreased hydrogen storage capacity. The grid was also studied when the wind power capacity increased and the continuous delivery to shore shortened. All intervals for continuous delivery: yearly, monthly, and 9.125 days, had many of the same tendencies. They had an increasing grid import and export transmission for a decreasing storage capacity. However, there were many hours of free capacity in the grid, allowing further utilisation for transmitting power for other purposes like, for example, a connection to an offshore grid. The amount of time the electrolyser produced hydrogen at its threshold value increased when the storage capacity decreased. The increase in the wind power capacity led to a decrease in the necessary hydrogen storage demand. The 10 % storage capacity cases were the only component combinations that imported power from the 2800 MW cases. It remains to weigh the economic aspects of the increased price of increased storage capacity, with the predictability of continuous delivery to the end-user for longer intervals. The upscaling of the wind power plant utilised the already invested components better, by exporting more power with the same grid capacity.

This thesis also aimed to investigate the potential subsea storage opportunities in the North Sea, and the salt cavern storage potential was studied. Analysis of the technical potential showed that only the Norwegian territory in the North Sea has the potential of storing 225,225,225 tons of working gas. Suppose a similar wind to hydrogen model with an integrated storage solution at the Southern North Sea that would utilise all of the storage potentials in the cavern and supply the shore with continuous hydrogen delivery. The wind to hydrogen model could have a total capacity of 39.57 TW. It would produce 128,080 TWh of hydrogen each year, five times the World's energy consumption. It remains to perform further technical analysis of the seabed to ensure the potential. Subsea operation of salt cavern hydrogen storage has not been operated before, and planned projects will collect meaningful experiences for establishing hydrogen storage in salt caverns.

References

[1] Alberto Toril Connor Donovan and Wilfred Yu. "Offshore Wind Outlook 2019". In: (2019).

[2] *Boosting Offshore Renewable Energy for a Climate Neutral Europe*. Accessed: 2022-05-30. 2020-11-19. URL: https://ec.europa.eu/commission/presscorner/detail/en/IP_20_2096.

[3] A. Sæbø et al. "Optimal utnyttelse av energi fra havvind i Nordlige Nordsjø II". In: (2021 [Online]. doi: https://greenstat.no/downloads/optimal-utnyttelse-av-energi-fra-havvind-i-sorlige-nordsjo-ii_hr-tn.pdf).

[4] *Storstilt satsing på havvind*. https://www.regjeringen.no/no/aktuelt/storstilt-satsing-pa-havvind/id2900436/. Accessed: 2022-05-04. Feb. 9, 2022.

[5] *Kraftfull satsing på havvind*. https://www.regjeringen.no/no/aktuelt/kraftfull-satsing-pa-havvind/id2912297/. Accessed: 2022-05-04. May 11, 2022.

[6] Dolf Gielen et al. "World Energy Transitions Outlook: 1.5° C Pathway". In: (2021).

[7] Jimena Incer-Valverde et al. "Power-to-liquid hydrogen: Exergy-based evaluation of a large-scale system". In: *International Journal of Hydrogen Energy* (2021).

[8] Ahmed M. Elberry et al. "Large-scale compressed hydrogen storage as parf renewable electricity storage systems". In: *International Journal of Hydrogen Energy* 46.29 (2021), pp. 15671–15690. ISSN: 0360-3199. DOI: https://doi.org/10.1016/j.ijhydene.2021.02.080. URL: https://www.sciencedirect.com/science/article/pii/S0360319921005838.

[9] Angeliki Spyroudi et al. "Offshore wind and hydrogen: solving the integration challenge". In: (2020).

[10] Energy and Climate Change Directorate. "Offshore wind to green hydrogen: opportunity assessment". In: *Scottish Government* (2020). URL: https://www.gov.scot/publications/scottish-offshore-wind-green-hydrogen-opportunity-assessment/documents/.

[11] Team Plan-AE et al. "Planning & Permitting study for North Sea Windpower Hub". In: (2019).

[12] Sheila Carreno-Madinabeitia et al. "Long-term changes in offshore wind power density and wind turbine capacity factor in the Iberian Peninsula (1900–2010)". In: *Energy* 226 (2021), p. 120364.

[13] Regjeringen Solberg. "Energi til arbeid – langsiktig verdiskaping fra norske energiressurser". In: *Det Kongelige Olje- og Energidepartementet* (June 11, 2021). Accessed: 2021-09-15.

[14] Thomas Hansen. "Havvind - enkelt forklart". In: *Universitetet i Bergen* (May 15, 2020). Accessed: 2021-05-15.

[15] Wenjie Zhou et al. "Simplified tz models for estimating the frequency and inclination of jacket supported offshore wind turbines". In: *Computers and Geotechnics* 132 (2021), p. 103959.

[16] Johns Hopkins University. URL: https://www.sciencedaily.com/releases/2011/01/110120111332.htm.

[17] Alfredo Ursua, Luis M. Gandia, and Pablo Sanchis. "Hydrogen Production From Water Electrolysis: Current Status and Future Trends". In: *Proceedings of the IEEE* 100.2 (2012), pp. 410–426. DOI: 10.1109/JPROC.2011.2156750.

[18] Mikhail Dvoynikov et al. "New Concepts of Hydrogen Production and Storage in Arctic Region". In: *Resources* 10.1 (2021), p. 3.

[19] David Berstad et al. "Liquid hydrogen as prospective energy carrier: A brief review and discussion of underlying assumptions applied in value chain analysis". In: *Renewable and Sustainable Energy Reviews* 154 (2022), p. 111772. ISSN: 1364-0321. DOI: https://doi.org/10.1016/j.rser.2021.111772. URL: https://www.sciencedirect.com/science/article/pii/S1364032121010418.

[20] A Peschel. "Industrial perspective on hydrogen purification, compression, storage, and distribution". In: *Fuel Cells* 20.4 (2020), pp. 385–393.

[21] Ulf Bossel. "Does a hydrogen economy make sense?" In: *Proceedings of the IEEE* 94.10 (2006), pp. 1826–1837.

[22] Ahmet Ozarslan. "Large-scale hydrogen energy storage in salt caverns". In: *International Journal of Hydrogen Energy* 37.19 (2012). HYFUSEN, pp. 14265–14277. ISSN: 0360-3199. DOI: https://doi.org/10.1016/j.ijhydene.2012.07.111. URL: https://www.sciencedirect.com/science/article/pii/S0360319912017417.

[23] Henrietta W. Langmi et al. "Chapter 13 - Hydrogen storage". In: *Electrochemical Power Sources: Fundamentals, Systems, and Applications*. Ed. by Tom Smolinka and Jurgen Garche. Elsevier, 2022, pp. 455–486. ISBN: 978-0-12-819424-9. DOI: https://doi.org/10.1016/B978-0-12-819424-9.00006-9. URL: https://www.sciencedirect.com/science/article/pii/B9780128194249000069.

[24] Dilara Gulcin Caglayan et al. "Technical potential of salt caverns for hydrogen storage in Europe". In: *International Journal of Hydrogen Energy* 45.11 (2020), pp. 6793–6805. ISSN: 0360-3199. DOI: https://doi.org/10.1016/j.ijhydene.2019.12.161. URL: https://www.sciencedirect.com/science/article/pii/S0360319919347299.

[25] Vigdis Olden. "HyLINE - Sikre rørledninger for hydrogentransport". In: *Sintef.no* (Nov. 22, 2019). Accessed: 2021-09-13.

[26] Glenn O Brown. "The history of the Darcy-Weisbach equation for pipe flow resistance". In: *Environmental and water resources history*. 2003, pp. 34–43.

[27] Polycarp Onyebuchi, Samuel Ugwu, and Udoka Opata. "A NOVEL LEAK DETECTION IN OIL PIPELINE USING MODIFIED DARCY-WEISBACH EQUATION". In: *International Journal of Scientific and Engineering Research* 9 (Aug. 2018), pp. 452–459.

[28] Norsk petrolium. "Rørtransportsystemer". In: *Norsk Petrolium* (Mar. 19, 2020). Accessed: 2021-09-28.

[29] *Detailed information on datasets*. https://www.renewables.ninja/downloads. Accessed: 2022-05-04.

[30] Iain Staffell and Stefan Pfenninger. "Using bias-corrected reanalysis to simulate current and future wind power output". In: *Energy* 114 (2016), pp. 1224–1239. ISSN: 0360-5442. DOI: https://doi.org/10.1016/j.energy.2016.08.068. URL: https://www.sciencedirect.com/science/article/pii/S0360544216311811.

[31] Magnus Korpås. "Distributed Energy Systems with Wind Power and Energy Storage". In: (). Doctoral thesis at NTNU 2004:39.

[32] Magnus Korpaas. *WindHydTool:Short Description*. Working Note. NTNU, Trondheim, 2004.

[33] eSubsea. *Subsea Ammonia and Hydrogen Storage*. https://www.esubsea.com/subsea-ammonia-and-hydrogen-storage/. Accessed: 2022-01-15.

[34] Gonçalo Calado and Rui Castro. "Hydrogen production from offshore wind parks: Current situation and future perspectives". In: *Applied Sciences* 11.12 (2021), p. 5561.

[35] Alain Le Duigou et al. "Relevance and costs of large scale underground hydrogen storage in France". In: *International Journal of Hydrogen Energy* 42.36 (2017), pp. 22987–23003. ISSN: 0360-3199. DOI: https://doi.org/10.1016/j.ijhydene.2017.06.239. URL: https://www.sciencedirect.com/science/article/pii/S0360319917326824.

[36] Andrew Lee. *Subsea caverns to store hydrogen from gigawatt-scale wind farms in 'world first' plan by Engie unit*. https://www.rechargenews.com/energy-transition/subsea-caverns-to-store-hydrogen-from-gigawatt-scale-wind-farms-in-world-first-plan-by-engie-unit/2-1-1132898. Accessed: 2022-02-07. Dec. 20, 2021.

[37] Kyrre Lundseth. *Grønn omstilling offshore*. https://www.sintef.no/siste-nytt/2021/gronn-omstilling-offshore/. Accessed: 2022-02-08. Jan. 8, 2021.

[38] TechnipFMC. *Energy Transition, Deep Purple™*. https://www.technipfmc.com/en/what-we-do/subsea/energy-transition-deep-purple/. Accessed: 2022-02-08.

[39] GCE Ocean Technology. *Subsea Energy Storage*. https://www.gceocean.no/news/posts/2018/september/subsea-energy-storage/. Accessed: 2022-02-08. Sept. 27, 2018.

[40] Silvio Matysik Lucas Bauer. *MHI Vestas Offshore V164-10.0MW*. https://en.wind-turbine-models.com/turbines/1912-mhi-vestas-offshore-v164-10.0mw. Accessed: 2021-10-21.

[41] SSE renewables. *Seagreen Offshore Wind Farm*. https://www.sserenewables.com/offshore-wind/projects/seagreen/. Accessed: 2022-05-06. 2020.

[42] Magnus Korpås. private communication.

[43] Anders Odegaard. *REFHYNE II will build the world's largest PEM electrolyser for hydrogen production – an important step towards GW-size electrolyse plants*. https://www.sintef.no/en/latest-news/refhyne-ii-will-build-the-worlds-largest-pem-electrolyser-for-hydrogen-production-an-important-step-towards-gw-size-electrolyse-plants/. Accessed: 2021-09-12. Oct. 8, 2021.

9 Appendix

9.1 Defining the constants

```
import matplotlib.pyplot as plt
import numpy as np

'''
All of the determined constants
'''
global L,T,delta,mu,R,M,D,P0,sH,JtoWh,EL,P,p,p_salt
T=283                           # [K]           temperature
L= 200*10**(3)                  # [m]           length of pipeline
delta=0.02*10**(-3)             # [m]           roughness pipeline
mu=0.84*10**(-5)                # [Pa s]        dyn. viscosity
R=8.314462175                   # [J K-1 mol-1] gas constant
Mm_H2=2.01594*10**(-3)          # [kg/mol]      molar mass
D=30*0.0254                     # [m]           diameter
p0=30*10**5                     # [bar]         pressure
sH=1.410                        # [dim.less]    specific heat ratio
P=1400                          # [MW]          power of wind park
eff_wind_toEL_offshore=0.97     # [%/100]
EL=0.052                        # [MWh/kgH2]    efficiency electrolysis
LHV=33.3*10**(-9)               # [TWh/kg]
p=100*10**5                     # [Pa] in pipeline
p_salt=180*10**(5)              # [Pa] in salt deposit
p_tank=350*10**(5)              # [Pa] in storage tanks
p_tank_future=700*10**(5)       # [Pa] in storage tanks
p_none=1                        # [Pa] to use Nm3 in the analysis
#conversion constant
JtoWh=0.000278 # Joule to Watt hour
# Hour interval when dividing the year in smaller intervals with constant
    delivery to shore
hourInterval=[ 24, 120, 219]#, 292, 365, 438]
```

9.2 Defining the functions

```
'''
```

```
All of the necessary functions to calculate simulate the wind to hydrogen power plant
'''
from doctest import ELLIPSIS_MARKER
from tkinter import CENTER
import numpy as np
import matplotlib.pyplot as plt
import math
from itertools import chain

def readFile(filename):
    '''
    Read the file with wind power data, and converts the information to an array
    '''
    all=[] #contain values between 0 and 1, which represent the cap.factor that hour
    count=0
    with open(filename+'.txt') as f:
        line = f.readline()
        line = f.readline()
        line = f.readline()
        line = f.readline()
        while line:
            line = f.readline()
            line=line.split(',')
            count+=1
            if line[len(line)-1]!='':
                all.append(float(line[len(line)-1])) # all=[MWh] and one element per hour per year
            if count>8764:
                break
        all=np.array(all)
    return all
def meancapyear_func(all):
    '''
    Calculate the mean capacity factor
    '''
    meanyear=sum(all)/len(all)
```

```
    meanyear=meanyear*100
    return meanyear
def plotMonthMean(all,meanyear):
    '''
    Plot the mean produced hydrogen, which is the demand at shore, and plot it
    .
    '''
    month=[31,28,31,30,31,30,31,31,30,31,30,31]          #days in a month
    month=np.array(month)
    month=24*month
    IM=0
    hour=0
    average=[]
    sum=0
    for elem in all: #iterating through all of the hours in a year
        hour+=1
        if hour==month[IM]:
            IM+=1
            average.append(sum/hour*1400)
            hour=0
            sum=0
        sum+=elem
    monthN=['Jan','Feb','Mar','Apr','May','June','July','Aug','Sep','Oct','Nov
    ','Dec']
    fig = plt.figure(figsize=(10, 5))
    plt.rcParams['font.size'] = '15'
    plt.rcParams["font.family"] = "Times New Roman"
    # annual average:
    meanyear_arr=np.zeros(len(average))
    meanyear_arr=meanyear_arr+meanyear/100*1400
    plt.plot(monthN,meanyear_arr,'-',color='coral',label='Yearly average')
    #monthly average:
    plt.plot(monthN,average,'-x',color='olivedrab',label='Montly average')
    plt.ylabel('Average power [MW]')
    plt.ylim(ymin=0,ymax=1400)
    plt.yticks(np.arange(0, 1500, 100))
    plt.grid()
    plt.xlabel('month')
    plt.legend()
```

```
    plt.savefig('monthmean.pdf')
    plt.show()
def E_compressFunc(p):
    '''
    Calculate the compression energy demand for compression form p0 to p
    '''
    V0=1/(p0*Mm_H2/(R*T))                                    # [m^3]
    W_ad=(sH/(sH-1))*p0*V0*((p/p0)**((sH-1)/sH)-1)*JtoWh    #adiabatic
    compression work
    W_iso=p0*V0*math.log(p/p0)*JtoWh                         #isothermal
    compression work
    E_compress=((W_ad-W_iso)/2+W_iso)*10**(-6)               #[MWh/kg]
    multistage compression work
    return E_compress
def kg_H2(all,eff_compr,EL):
    '''
    Calculate the hydrogen produced each hour in the wind power plant with
    power curve - all
    '''
    EL_pluss_eff_compr=EL+eff_compr                          # MWh/kg used in
    electrolysis and compression
    kgH2=all/EL_pluss_eff_compr                              # multiply
    elementwise - result is an array with kg H2 each day
    return kgH2
def headLossFunc(p,kg_H2_arr):
    '''
    Calculate the pressure head loss, the pressure drop when transporting
    hydrogen through a pipeline
    '''
    ro_100=p*Mm_H2/(R*T)       # [kg/m^3], density at p bar
    A=(math.pi/4)*D**2      # [m^2] area in the pipeline
    eta=delta/D             # [dim.less] rel. roughness
    V=kg_H2_arr/ro_100      # [m^3] array with hourly volume of H2 at 100
    pascal
    v=V/A/3600              # [m/s] velocity of the H2 in the pipeline
    Re_array=v*D*ro_100/mu  # [dim.less] array of the hourly Reynoldsnumber
    dP_list=[]
    count=0
    headLoss=0
```

```
    for re in Re_array:         #iterating through the Reynoldsnumbers
        if re>2000:             #if turbulent
            f=(-2*math.log((eta/3.7)+(5.74/(re**(0.9))),10))**(-2) #
    calculating the friction factor
        elif re<2000 and re>0: #if laminar
            f=64/re
        else:
            print('error!')
        headLoss=f*L*v[count]**2/(2*9.81*D)    #calculating friction head loss
        dP=headLoss*ro_100*9.81
        dP_list.append(dP)
        count+=1
    dP_list=np.array(dP_list)
    meandP=sum(dP_list)/len(dP_list)*10**(-5)  #[bar] calculating the yearly
    mean pressure drop
    return meandP,dP_list
def ALL(all,p):
    '''
    Defining the wind power capacity array, from the capacity array - all
    '''
    allW=all*P*eff_wind_toEL_offshore        # [MW] incert power to
    electrolysis

    E_compress=E_compressFunc(p)             # [MWh/kgH2] calculate
    compression energy demand
    kg_H2_arr=kg_H2(allW,E_compress,EL)      # [array] elements with kg H2
    kg_H2_meanYear=np.mean(kg_H2_arr)        # Mean produced hydrogen each
    hour
    return kg_H2_arr,kg_H2_meanYear
def ALL_storage(all,p,Power):
    '''
    Calculate the wind power function and the hydrogen produced in one
    function
    '''
    allW=all*Power*eff_wind_toEL_offshore        # [MW] incert power to
    electrolysis
    E_compress=E_compressFunc(p)             # [MWh/kgH2]
    kg_H2_arr=kg_H2(allW,E_compress,EL)      # [array] elements with kg H2
    kg_H2_meanYear=np.mean(kg_H2_arr)
```

```
137     return kg_H2_arr,kg_H2_meanYear
138 def plotMeanKgH2(kg_H2_arr):
139     '''
140     plot the mean hydrogen produced
141     '''
142     kg_H2_meanYear=np.mean(kg_H2_arr)
143     x=np.linspace(0,len(kg_H2_arr),len(kg_H2_arr))
144     plt.plot(x,kg_H2_arr)
145     kg_H2_meanYear_arr=np.full_like(x,kg_H2_meanYear)
146     plt.plot(x,kg_H2_meanYear_arr)
147     plt.show()
148 def get_storage(kg_H2_arr):
149     '''
150     Calculate the storage status for a yearly constant demand at shore
151     '''
152     storage=[]
153     kgH2ToShore=np.mean(kg_H2_arr)
154     for h2 in kg_H2_arr:
155         storage.append(h2-kgH2ToShore)
156     storage=np.array(storage)
157     storage_status=np.cumsum(storage)
158     return storage_status
159 def check_storage_season(kg_H2_arr):
160     '''
161     Calculate the storage status for a monthly constant demand at shore
162     '''
163     fig, ax = plt.subplots(figsize=(18, 8))
164     plt.rcParams.update({'font.size': 20})
165     fs=24 #fontsize
166     month=[31,28,31,30,31,30,31,31,30,31,30,31]          #days in a month
167     month=np.array(month)
168     month=24*month #month array with hour that month in every element
169     monthN=['Jan','Feb','Mar','Apr','May','June','July','Aug','Sep','Oct','Nov
    ','Dec']
170     count=0
171     monthStart=0
172     storage_s=[]
173     storage_s_status=[] #
174     monthCount=0        #
```

```
    mean=[]
    s_store_max=0
    ALLstorage=[]
    store_min=0
    tot_store_min=0
    store_max=0
    tot_store_max=0
    STORAGE_GATHER=[]
    for M in month:
        storage_s_status=[]
        storage_s=[]
        monthMean=np.mean(kg_H2_arr[monthStart:monthStart+M])
        mean.append(monthMean)
        for hour in range(M):
            storage_s.append(kg_H2_arr[count]-monthMean)
            count+=1
        storage_s_status=np.cumsum(storage_s)
        STORAGE_GATHER.append(storage_s_status)
        ALLstorage.append(storage_s_status)
        monthCount+=1
        monthStart+=M
        store_min=np.min(storage_s_status)
        if store_min<tot_store_min:
            tot_store_min=store_min
        elif tot_store_max<store_max:
            tot_store_max=store_max
    STORAGE_GATHER=list(chain.from_iterable(STORAGE_GATHER))
    STORAGE_GATHER=np.array(STORAGE_GATHER)-tot_store_min
    monthStart=0
    monthCount=0
    count=0
    for M in month:
        monthMean=mean[count]
        x=np.linspace(monthStart,monthStart+M,M)
        ax.plot(x,np.zeros(len(x)),'--',linewidth=3,color=colors_plot[0])
        ax.plot(x,STORAGE_GATHER[monthStart:monthStart+M]/1000,label=monthN[
monthCount]+', '+str(round(monthMean/1000,1))+' tons/h',linewidth=3,color=
colors_plot2[monthCount])
        monthCount+=1
```

```
        monthStart+=M
        count+=1
    box = ax.get_position()
    ax.set_position([box.x0, box.y0, box.width * 0.8, box.height])
    x=np.linspace(0,len(kg_H2_arr),len(kg_H2_arr))
    monthplot=np.cumsum(month)-0.5*month
    monthplot_min=np.cumsum(month)
    #month=interval_func(month)
    ax.set_xticklabels(monthN,fontsize=fs)
    ax.set_xticks(monthplot)
    ax.set_xticks(monthplot_min,minor=True)
    plt.ylabel('H2 stored [tons]',fontsize=fs)
    plt.yticks(fontsize=fs)
    ax.set_yticks(np.arange(-500,2400,200))
    ax.set_xlim(0,len(kg_H2_arr))
    ax.grid(which='both')
    ALLstorage=list(chain.from_iterable(ALLstorage))
    ALLstorage.sort(reverse=True)
    ALLstorage=np.array(ALLstorage)-tot_store_min
    ax.plot(x,ALLstorage/1000,label='duration curve',zorder=0,color='gainsboro
    ',linewidth=3)
    s_store_max=np.max(ALLstorage)
    plt.legend(loc='center left', bbox_to_anchor=(1, 0.5))
    plt.rc('xtick', labelsize=fs)
    plt.rc('ytick', labelsize=fs)
    plt.savefig('_saved_monthmean.pdf', bbox_inches='tight')
    plt.show()
    calc_salt_and_tank(s_store_max)

    return storage_s_status,ALLstorage,mean


def check_storage_10days(kg_H2_arr, interval_in): # interval_in needs to be in
    hours
    '''
    Calcualte storage deposit for interval_in length of the interval
    '''

    if int(len(kg_H2_arr))%interval_in==0:
```

```
        s_store_max=0
        store_min=0
        s_store_min=0
        storage_s=[]
        storage_s_status=[]
        mean=[]
        intervalcount=len(kg_H2_arr)/interval_in
        intervalcount=int(intervalcount) #how many times is the interval going
    to loop?
        ALLstorage=[]
        for count in range(0,intervalcount):
            hourStart=interval_in*count
            storage_s_status=np.array([])
            storage_s=np.array([])
            arr=kg_H2_arr[hourStart:(hourStart+interval_in)]
            mean_int=np.mean(arr)
            mean.append(mean_int)
            storage_s=arr-mean_int
            storage_s_status=np.cumsum(storage_s)
            store_max=np.max(storage_s_status)-np.min(storage_s_status)
            store_min=np.min(storage_s_status)
            if store_max>s_store_max:
                s_store_max=store_max
            if store_min<s_store_min:
                s_store_min=store_min
            ALLstorage.append(storage_s_status)
        print(mean)
        ALLstorage=list(chain.from_iterable(ALLstorage))
        ALLstorageSORT=ALLstorage.copy()
        ALLstorageSORT.sort(reverse=True)
        ALLstorage=np.array(ALLstorage)
        ALLstorageSORT=np.array(ALLstorageSORT)
        V_max_salt,V_max_tank=calc_salt_and_tank(s_store_max)
        return V_max_salt,V_max_tank,s_store_max,ALLstorageSORT,ALLstorage,
    s_store_min
    else:
        print('the interval is not dividable on 8760!')


```

```
286
287 def ALL_pipelineTransport(all,p,p_shore):
288     '''
289     Calculate the hydrogen gas created and accounting for the pressure loss in
        the pipeline
290     '''
291     allW=all*P*eff_wind_toEL_offshore        # [MW] incert power to
    electrolysis
292
293     E_compress=E_compressFunc(p)              # [MWh/kgH2]
294
295     kg_H2_arr=kg_H2(allW,E_compress,EL)       # [array] elements with kg H2
296
297     meandP,_=headLossFunc(p,kg_H2_arr)
298
299     if p*10**(-5)-meandP<p_shore*10**(-5): #pressure at the other side is to
    be 100 bar
300         meandP,kgH2_year,p=ALL(all,P,D,p+meandP*(10**5)*0.5,Mm_H2,R,T,
    eff_wind_toEL_offshore,EL,mu,p0,sH,L,delta)
301     return meandP,kgH2_year,p
302
303
304
305 def storage_capacity(Power,p,all):
306     '''
307     returns the total amount of storage capacity
308     '''
309     kg_H2_arr,_=ALL_storage(all,p,Power)
310     storage_status=get_storage(kg_H2_arr)
311     max_storage_capacity=np.max(storage_status)-np.min(storage_status)
312     return max_storage_capacity,kg_H2_arr #[kg]
313
314
315 def V_calc(m_workingGas):
316     '''
317     Calculate the volume of a salt cavern which stores m_working gas
318     '''
319     depth=1200          #[m]
320     cavern_height=120   #[m]
```

```
    Z=1.2
    ro_rock=2700
    P_overburden=ro_rock*9.81*(depth-cavern_height)
    ro_max=0.80*P_overburden*Mm_H2/(Z*R*T)
    ro_min=0.24*P_overburden*Mm_H2/(Z*R*T)
    Theta_safety=0.70 #[%]
    V_cavern_tot=m_workingGas/((ro_max-ro_min)*Theta_safety)
    return V_cavern_tot

def calc_salt_and_tank(store_max):
    '''
    Calculate the volume of a salt cavern and a pressure tank which stores
    store_max
    '''
    V_max_salt=(store_max*R*T)/(p_salt*Mm_H2)
    V_max_tank=(store_max*R*T)/(p_tank*Mm_H2)
    return V_max_salt,V_max_tank
```

9.3 Calculating the wind to hydrogen power plant

```
'''
Simulate the wind to hydrogen power plant
'''

import matplotlib.pyplot as plt
import numpy as np

''' Import weather data'''

all=readFile('SN2_MHIVestasV164_10MW_mKoordTXT')        # import the text from
    renewables.ninja file
meanyear=meancapyear_func(all)                          # [%] mean cap factor
plotMonthMean(all,meanyear)                            # plot mean capacity
    factor
```

9.4 Calculate the storage status of yearly constant intervals

```

'''
```

```
Calculating and plotting the storage situation with a constant delivery to
    shore through the whole year.
'''

kg_H2_arr,kg_H2_meanYear=ALL(all,p0)

storage_status=get_storage(kg_H2_arr)
```

9.5 Calculate the storage status of monthly, 9.125 days, 5 days and 1 day constant intervals

```
'''
Calculating the case with various intervals
'''

# wind power to produced hydrogen
kg_H2_arr,kg_H2_meanYear=ALL(all,p0)

ALLstorage=[]
labels=[]
Salt=[]
Tank=[]
Kgstored=[]

#storage montly interval:
storage_s_status,ALLstoragemonth,mean=check_storage_season(kg_H2_arr) #
    monthly
max_m=np.max(ALLstoragemonth)
Kgstored.append(max_m)
V_salt_m,V_tank_m=calc_salt_and_tank(max_m)


# distinct days intervals:
x=np.linspace(0,8760,8760)
for int in hourInterval[::-1]:
    salt,tank,_,ALLstoragehour,ALLstorage_array,_=check_storage_10days(
    kg_H2_arr,int)
    Salt.append(salt)
    Tank.append(tank)
    Kgstored.append(np.max(ALLstoragehour)-np.min(ALLstoragehour))
```

```
    ALLstorage.append(ALLstoragehour)
    labels.append(str(round(int/24,2))+' days interval')


'''
Calculating the salt cavern potential in Norway
'''
CavernCapacity_Norway=7500     #[TWh]

m_workingGas=CavernCapacity_Norway/LHV     # [kg] total mass of hydrogen which
    can be stored

V_cavern_tot=V_calc(m_workingGas)           #[m^3] volume of the salt cavern

''' Iterating through to find the potential storage oppurtunity in the salt
   cavern '''

P=1400 # [MW]
max_storage_capacity,kg_H2_arr=storage_capacity(P,p_salt,all)
while max_storage_capacity<m_workingGas:
    P+=1 #[MW]
    max_storage_capacity,kg_H2_arr=storage_capacity(P,p_salt,all)

Area=(7*164)**2*P/10 # Total amount of area needed to establish a wind power
   plant of capacity, P
```

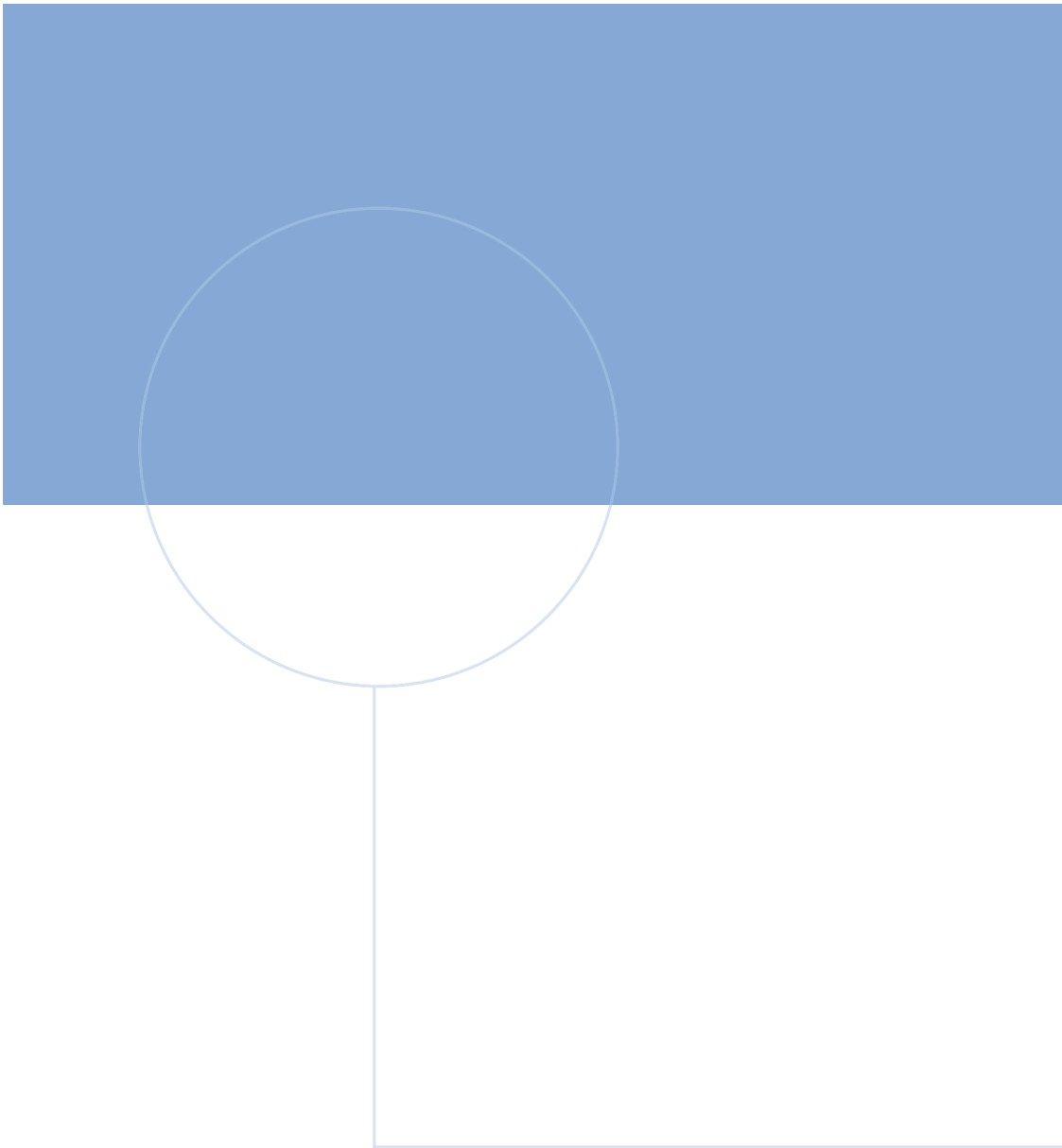

NTNU

Norwegian University of
Science and Technology